AD-A099 995 AEROSPACE CORP EL SEGUNDO CA LAB OPERATIONS F/G 11/3
MULTICOMPONENT OXIDE SYSTEMS FOR CORROSION PROTECTION,(U)
NOV 80 G W STUPIAN, P D FLEISCHAUER AFOSR-77-3334
UNCLASSIFIED ATR-81(7679)-1 AFOSR-TR-81-0472 NL

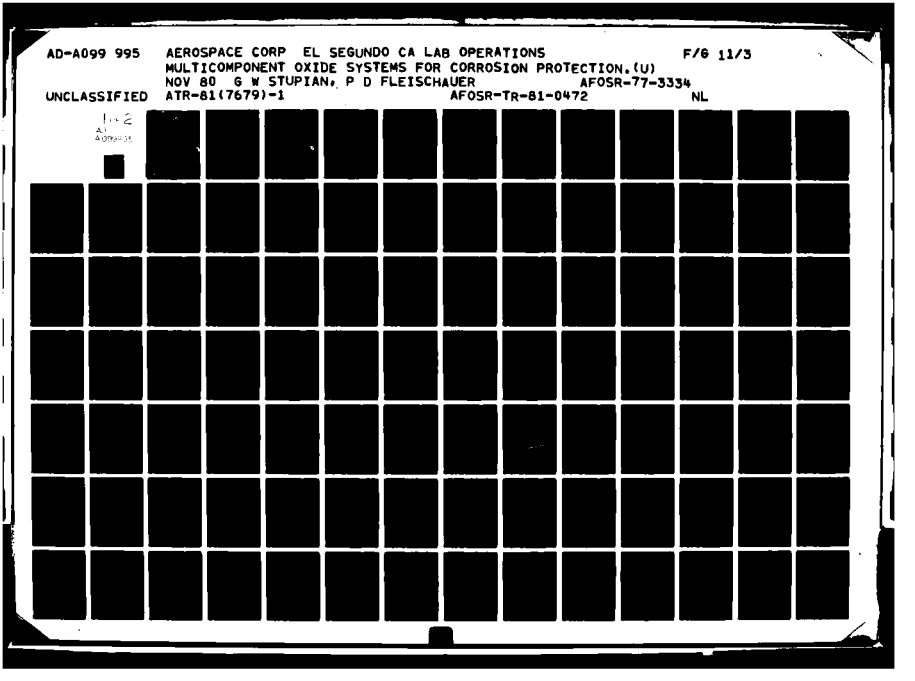

AEROSPACE REPORT NO.
ATR-81(7679)-1

LEVEL II

12

Final Report
Multicomponent Oxide Systems for Corrosion Protection

Prepared by

G. W. STUPIAN and P. D. FLEISCHAUER
Chemistry and Physics Laboratory
The Aerospace Corporation

15 November 1980

Prepared for

UNIVERSITY OF SOUTHERN CALIFORNIA
Los Angeles, California 90007

Purchase Order No. 40055

Laboratory Operations
THE AEROSPACE CORPORATION

LABORATORY OPERATIONS

The Laboratory Operations of The Aerospace Corporation is conducting experimental and theoretical investigations necessary for the evaluation and application of scientific advances to new military concepts and systems. Versatility and flexibility have been developed to a high degree by the laboratory personnel in dealing with the many problems encountered in the Nation's rapidly developing space systems. Expertise in the latest scientific developments is vital to the accomplishment of tasks related to these problems. The laboratories that contribute to this research are:

Aerophysics Laboratory: Aerodynamics; fluid dynamics; plasmadynamics; chemical kinetics; engineering mechanics; flight dynamics; heat transfer; high-power gas lasers, continuous and pulsed, IR, visible, UV; laser physics; laser resonator optics; laser effects and countermeasures.

Chemistry and Physics Laboratory: Atmospheric reactions and optical backgrounds; radiative transfer and atmospheric transmission; thermal and state-specific reaction rates in rocket plumes; chemical thermodynamics and propulsion chemistry; laser isotope separation; chemistry and physics of particles; space environmental and contamination effects on spacecraft materials; lubrication; surface chemistry of insulators and conductors; cathode materials; sensor materials and sensor optics; applied laser spectroscopy; atomic frequency standards; pollution and toxic materials monitoring.

Electronics Research Laboratory: Electromagnetic theory and propagation phenomena; microwave and semiconductor devices and integrated circuits; quantum electronics, lasers, and electro-optics; communication sciences, applied electronics, superconducting and electronic device physics; millimeter-wave and far-infrared technology.

Materials Sciences Laboratory: Development of new materials; composite materials; graphite and ceramics; polymeric materials; weapons effects and hardened materials; materials for electronic devices; dimensionally stable materials; chemical and structural analyses; stress corrosion; fatigue of metals.

Space Sciences Laboratory: Atmospheric and ionospheric physics, radiation from the atmosphere, density and composition of the atmosphere, aurorae and airglow; magnetospheric physics, cosmic rays, generation and propagation of plasma waves in the magnetosphere; solar physics, x-ray astronomy; the effects of nuclear explosions, magnetic storms, and solar activity on the earth's atmosphere, ionosphere, and magnetosphere; the effects of optical, electromagnetic, and particulate radiations in space on space systems.

UNCLASSIFIED

SECURITY CLASSIFICATION OF THIS PAGE (When Data Entered)

REPORT DOCUMENTATION PAGE

READ INSTRUCTIONS BEFORE COMPLETING FORM

1. REPORT NUMBER: AFOSR-TR-81-0472	2. GOVT ACCESSION NO.: AD-A099995
	3. RECIPIENT'S CATALOG NUMBER
4. TITLE (and Subtitle): MULTICOMPONENT OXIDE SYSTEMS FOR CORROSION PROTECTION.	5. TYPE OF REPORT & PERIOD COVERED: Final rept.
	6. PERFORMING ORG. REPORT NUMBER
7. AUTHOR(s): G. W. Stupian and P. D. Fleischauer	8. CONTRACT OR GRANT NUMBER(s): AFOSR-77-3334
9. PERFORMING ORGANIZATION NAME AND ADDRESS: University of Southern California, Graduate Center for Engineering & Computer Science, Los Angeles, Calif. 90007	10. PROGRAM ELEMENT, PROJECT, TASK AREA & WORK UNIT NUMBERS: 61102F, 2303/A2
11. CONTROLLING OFFICE NAME AND ADDRESS: Air Force Office of Scientific Research, AFOSR/NC, Bolling AFB, DC 20332	12. REPORT DATE: 15 November 1980 13. NUMBER OF PAGES: 104
14. MONITORING AGENCY NAME & ADDRESS (if different from Controlling Office)	15. SECURITY CLASS. (of this report): Unclassified 15a. DECLASSIFICATION/DOWNGRADING SCHEDULE

16. DISTRIBUTION STATEMENT (of this Report)

Approved for public release; distribution unlimited.

17. DISTRIBUTION STATEMENT (of the abstract entered in Block 20, if different from Report)

18. SUPPLEMENTARY NOTES

19. KEY WORDS (Continue on reverse side if necessary and identify by block number)

Aluminum Corrosion
Auger Electron Spectroscopy
Protective Oxides

20. ABSTRACT (Continue on reverse side if necessary and identify by block number)

The formation and function of corrosion-resistant surface oxide films on aluminum have been investigated during a three-year research effort. "Mixed" oxide coatings should, based on a conceptual model, offer superior corrosion resistance (a mixed oxide is defined as an oxide system based on more than one cation species). The structures of the mixed oxide coatings studied were characterized using Auger electron spectroscopy, x-ray photoelectron spectroscopy, and ion microprobe mass analysis. Corrosion resistance was assessed by exposing specimens in a salt chamber.

DD FORM 1473 (FACSIMILE)

UNCLASSIFIED 009575

19. KEY WORDS (Continued)

20. ABSTRACT (Continued)

Chromate coating systems, long in use on aluminum, were examined first to provide a standard against which to measure coating performance. Chromate coating formation was explained in terms of the role of hydrogen fluoride (or hydroxyl ion) in the dissolution of the native aluminum oxide layer and through the influence of the slight solubility difference between chromium and aluminum hydroxides on film growth.

New types of mixed oxide coatings deposited from nonaqueous solutions of organometallic compounds were developed. Titanium-aluminum mixed oxide coatings, deposited from solutions of titanium alkoxides in isopropanol, served as a prototype system for much of this work. It was found that the application of certain sulfur compounds in conjunction with titanate coatings resulted in enhanced corrosion resistance, and in one case (AA 6061), the corrosion resistance exceeded that of the chromate coatings. The feasibility of the basic approach taken here has been validated. It remains for future work to effect further improvements in the technique.

Report No.
ATR-81(7679)-1

FINAL REPORT

MULTICOMPONENT OXIDE SYSTEMS FOR CORROSION PROTECTION

Prepared

G. W. Stupian

P. D. Fleischauer

Approved

S. Feuerstein, Head
Interfacial Sciences Department

S. Siegel, Director
Chemistry and Physics Laboratory

ACKNOWLEDGMENTS

This work was supported by the Air Force Office of Scientific Research under Grant No. [redacted]. AFOSR-77-3334

Professional personnel associated with the program effort employed through the University of Southern California as postdoctoral researchers were: Howard A. Katzman, June 1977 through April 1978; George M. Malouf, August 1977 through October 1978; Russell A. Lipeles, January 1979 through October 1979; Frank E. Hanson, April 1979 through August 1979; and James A. Doi, October 1979 through September 1980.

Also, Ted H. Lee, B.S., was employed as a research assistant from April through September 1980.

The Aerospace Corporation personnel associated with the program from inception to the end of the program were the principal investigator, Dr. Gary W. Stupian and Dr. Paul D. Fleischauer, Section Manager, Surface Chemistry. Mr. Reinhold Bauer assisted with the experimental work during the early stages of the program. The authors also wish to extend special thanks to Armond B. Chase of the Aerospace Electronics Research Laboratory for many useful and stimulating technical discussions.

CONTENTS

FIGURES

FIGURES (Continued)

TABLES

I. INTRODUCTION

A three-year study of the potential of mixed oxide systems for the corrosion protection of aluminum alloys has been completed successfully. This report presents the results obtained during the three years of program effort. For the convenience of the reader, necessary background information is incorporated including the conceptual rationale, as presented in the original proposal, that led to the investigation of mixed oxide systems as anticorrosion coatings. Detailed accounts of most of the results obtained during the first two years of program effort have been published in the open literature (Refs. 1, 2). The present report provides, however, a complete recapitulation of the work as well as an account of progress in the final year.

The economic consequences of corrosion to the Air Force, and to other branches of the government and to industry, are substantial. The Air Force must, in addition, be concerned with the impact of corrosion-related problems on mission readiness and on personnel safety. Aircraft aluminum surfaces are currently partially protected against corrosion by the use of chromate coatings and by paints. A degree of corrosion protection is certainly afforded by the available technologies; nevertheless, improved corrosion resistance could still result in substantial cost avoidance. Commercial airlines have begun again to leave aircraft unpainted because of the fuel penalty incurred by the weight of the paint. Oxide coatings are much thinner and, therefore, much lighter.

All structural metals are thermodynamically unstable under ordinary conditions of temperature and pressure with respect to the formation of their oxides. Metals exist, as such, only because the surface oxide layers initially formed may decrease the rate of further oxidation, i.e., metals are kinetically, but not thermodynamically, stable. The interaction of a metal with the environment is thus a reaction of a metal oxide with the environment. A detailed understanding of the oxide-ambient interface is essential to the resolution of many fundamental and practical problems, including the prevention and control of metallic corrosion.

Our research effort was founded on a conceptual model of the protective oxide layer on a metal surface. This model predicts that mixed oxides should afford better corrosion protection than native surface oxides. A mixed oxide is defined here simply as an oxide system containing more than one cation species. The chromate coatings now in use for the protection of aluminum alloys are mixed oxide systems. We have performed a detailed study of mixed oxide coatings on aluminum to develop more effective protective coatings.

The original research was divided into three tasks (Ref. 3). Task A involved the evaluation of composition versus corrosion resistance for commercial chromate coating formulations and was largely completed during the first year of the program. Our work constituted the most thorough investigation to date of the chromate-aluminum system using modern techniques of surface analysis (Refs. 1, 4).

The second and third years of program effort involved Task B, the development of new techniques for the deposition of mixed oxide coatings from nonaqueous solutions of organometallic compounds (Refs. 2, 5). Much of the experimental work involved titanium-aluminum mixed oxide films, and work on this model system resulted in a much clearer picture of the formation and function of corrosion-resistant mixed oxide layers. Other oxide systems were also examined. Corrosion resistance of the titanate and other oxide coatings was in general inferior to that of the chromate coatings. We did, however, succeed in the development of a coating involving a titanate for a particular aluminum alloy (AA 6061) that exhibited better corrosion resistance than commercial chromate coating formulations. This work points the way toward further research.

Task C involved recommendations of corrosion-protective processes suitable for practical application to aircraft. Only preliminary recommendations are possible at this time, but it is important to note that the feasibility of coating solution deposition involving primarily substitution reactions as opposed to redox reactions has been demonstrated.

II. EXPERIMENTAL PROCEDURES

Certain experimental techniques common to all phases of our work are summarized in this section.

A. SURFACE ANALYSIS TECHNIQUES

Deposited coatings were characterized using several modern analytical methods for surface analysis. These techniques have been widely described in the literature and need only be mentioned briefly.

1. AUGER ELECTRON SPECTROSCOPY

Most of our experimental characterization of coatings has been accomplished using Auger electron spectroscopy (AES) (Ref. 6). In AES, an incident electron beam (with an energy typically 2 to 5 keV) excites secondary electron emission from the specimen surface. Auger processes in emitting atoms give rise to electrons with characteristic, known kinetic energies, and energy analysis of the secondary electron distribution thus provides an elemental analysis of the specimen surface. Auger electron spectroscopy will, in general, indicate the presence of any element with a surface concentration greater than about 0.1 to 1.0% of a surface monolayer. Elemental concentrations are derived from experimental Auger spectra using a standard method that, while subject to some errors, is accurate to perhaps 10% and is in wide use (Ref. 7).

Auger spectroscopy is a surface analysis technique because of the very short mean free path for inelastic scattering characteristic of electrons in solids in the 20 to 2000 eV range. Auger electron spectroscopy detects only those elements present in the outer three to four atomic layers of the specimen surface.

Much of our work necessitated the determination of specimen composition as a function of depth into the specimen. This information was obtained by combining Auger analysis with simultaneous ion etching. A multiplex device permits automatic recording of the peak-to-peak heights (taken as a measure of concentration) of up to six elements and plotting of these peak heights as a

function of sputtering time. The sputter rate is assumed to be constant, and sputter time is related to depth beneath the specimen surface by suitable calibration. In our work, Ta_2O_5 anodic oxide films of accurately known thickness were employed as calibration standards.

A Physical Electronics Industries Model 10-150 cylindrical-mirror Auger spectrometer was used in most of the experiments described here. This instrument provides for a maximum incident electron-beam energy of 5 keV and has an energy resolution ($\Delta E/E$) of about 0.6%. The system vacuum chamber typically operated in the 10^{-9} Torr pressure range. A Physical Electronics Industries Model 590 scanning Auger microprobe was used for some measurements.

2. X-RAY PHOTOELECTRON SPECTROSCOPY

X-ray photoelectron spectroscopy (XPS, also known by the acronym ESCA) was also used to some extent in our investigation. In XPS, an incident x-ray beam excites photoelectrons from the test specimen (Ref. 6). The photoelectron kinetic energies of interest in XPS are roughly the same as the electron kinetic energies found in AES, and XPS is thus also a surface-sensitive technique. Semiquantitative elemental analysis is possible with XPS; however, photoelectron emission is basically a simpler process than Auger electron emission and permits a direct measurement of the binding energy of an electron in an atom. The binding energy is dependent upon the environment of the atom, i.e., on its bonding to its neighbors. X-ray photoelectron spectroscopy thus directly yields information on chemical bond formation, and we have made use of this capability. Auger electron spectroscopy and XPS have additional relative advantages and disadvantages that have been discussed in Ref. 6.

The instrument employed in our studies was a McPherson Instruments Model ESCA 36 using Mg Kα exciting radiation.

3. ION MICROPROBE MASS ANALYZER

The ion microprobe mass analyzer (IMMA) subjects a specimen to an incident ion beam (usually of O^- ions), and performs a mass/charge ratio analysis of species arising from the specimen surface (Ref. 8). The sputtered mass

spectrum is quite complex, since chemical reactions take place between specimen atoms and the incident oxygen atoms. The IMMA is, however, considerably more sensitive than AES or XPS to certain species in bulk, and we have used this fact to our advantage. The IMMA method is conceptually identical to secondary ion mass analysis (SIMS). The Applied Research Laboratories instrument available in our laboratory happens to be an imaging mass analyzer capable of providing about 2-μm spatial resolutions parallel to the surface.

B. CORROSION-RESISTANCE EVALUATION

Coating corrosion resistance was assessed semiquantitatively by exposing test coupons in a salt-fog chamber (Associated Testing Laboratories Model SS-3-8) operated with a 50% NaCl solution at 35°C and 100% relative humidity. Coupons were examined at regular intervals and rated on an arbitrary visual corrosion scale from 0 to 6 in half-unit steps. The time interval required for the onset of visible corrosion proved to be a useful measure of relative corrosion resistance. Some experiments were conducted to assess the possibility of better quantifying corrosion resistance using electrochemical techniques; however, the salt spray method was deemed adequate for our purposes.

III. BACKGROUND DISCUSSION

A. CONCEPTUAL MODEL FOR CORROSION

Our goal was to gain a better understanding of the chemical and physical properties of surface oxide layers in order to form oxide layers on aluminum that offers a high degree of corrosion resistance. A brief general discussion of some properties of oxides is desirable to clarify the rationale behind the approach taken in our work. In particular, we should first inquire as to what is meant when an oxide is said to be stable.

The term "stability" is used in two distinct senses in describing chemical compounds. Stability sometimes is used to imply high bond strengths, i.e., a high melting temperature, and sometimes refers to resistance to chemical attack. These two meanings of stability are not synonymous. Many compounds with a low melting temperature are chemically unreactive, and vice versa. In this discussion, we consider an oxide to be stable if it is resistant to environmental chemical attack. Stability in the thermal sense is not of primary importance provided that the melting temperature of oxides considered is sufficiently high that thermal diffusion or decomposition under any reasonably anticipated operation conditions is precluded. As a general rule, these conditions are satisfied if the absolute oxide melting temperature is greater than twice the maximum temperature anticipated during use of the metal in question.

An oxide will be stable only over some particular range of environmental conditions. For practical problems of aircraft corrosion protection, one must consider an aluminum surface covered with a layer of water containing dissolved impurities. Depending on local conditions, the water film on the skin of an aircraft will range in pH from moderately alkaline to moderately acidic. We were concerned with developing corrosion inhibiting oxide films that function effectively in this intermediate pH range.

Some general criteria for assessing oxide corrosion resistance were needed to guide our investigation. The problem is perhaps best approached by

first asking what characteristics might be expected to render an oxide vulnerable to chemical attack, and by then requiring the opposite characteristics. Our criteria for corrosion resistance are discussed in detail in succeeding paragraphs. Naturally, an effective protective oxide will not necessarily satisfy all of these requirements simultaneously, although some requirements, such as the uniformity of the oxide films, are in fact necessary conditions for corrosion protection.

1. LOW ELECTRONIC CONDUCTIVITY

Increased availability of conduction electrons in a compound is associated with increased chemical reactivity. This fact is verified by experiments both in heterogeneous catalysis and in electrochemistry. Low electrical conductivity is therefore essential in a corrosion-resistant oxide. Oxides may exhibit both intrinsic and extrinsic semiconductivity. Low intrinsic conductivity is synonymous with a wide band gap. Extrinsic conductivity in an oxide results from impurities or through departures from stoichiometry. Both impurities and departures from stoichiometry result in the introduction of extra charge carriers into the oxide. Departures from stoichiometry are facilitated if the cations in an oxide are capable of existing in more than one valence state. In such cases, an oxygen atom can be removed from the material, which results in an oxygen vacancy, and charge neutrality is maintained by the concomitant reduction or partial reduction of a metal ion.

2. LOW IONIC CONDUCTIVITY

Ionic transport through an oxide film (as well as electron transport previously mentioned) can result in chemical reaction and thus implies that the oxide is not protective. If ionic transport is to be minimized, certain constraints are placed on the oxide crystal structure. Structures in which channels exist and permit easy migration of ions are necessarily precluded. In general, one would anticipate that greater covalent bond character in an oxide implies less easy cation migration since covalent bonds are directional and movement of a covalently bonded atom requires breaking of these directed bonds and a correspondingly large expenditure of energy. Tetrahedral coordination of the cation (i.e., four oxygen neighbors about each cation in the

directions of the vertices of a circumscribed tetrahedron, similar to SiO_2) is the crystal symmetry most closely associated with covalent bonding. In transition metal oxides, the cation is generally octahedrally coordinated, although half of the cation sites in the common spinel structure are tetrahedral. As a general rule, one concludes that tetrahedral bonding would be desirable. Octahedral coordination would be the next most satisfactory atomic arrangement.

3. LOW SOLUBILITY

Low solubility over the pH range of interest is required for a protective oxide. The implications of this fact will be discussed in greater detail in succeeding paragraphs.

4. PROPER COORDINATION WITH SUBSTRATE METAL

A protective oxide must easily form coordinate bonds with the substrate metal either as in a solid solution or through the formation of a stable compound. This bonding requirement is essential if the oxide is to form a continuous film. A continuous surface film is necessary if an oxide is to be protective; discontinuities expose reactive metal atoms. Continuity of the surface oxide film also ensures mechanical stability, i.e., resistance to abrasion and flaking. The existence of a close-packed plane of surface oxygen atoms greatly facilitates oxide-substrate bonding since both the substrate and the surface oxide layer can share a common oxygen plane. Oxide crystal lattices that have a closed-packed surface plane of oxygens will exhibit higher relative stability in an oxidizing environment.

The criteria previously presented do not constitute a set of completely independent requirements. For example, the crystal structure adopted by an oxide is connected with metal-oxygen bond ionicity. Nevertheless, in summary, these criteria provided a useful conceptual framework within which we considered the problem of oxide stability and corrosion protection.

B. EXAMPLES OF PRESENTLY USED PROTECTIVE OXIDE COATINGS

Metals are normally covered with a thin oxide film, typically about 40 Å thick. This film provides some corrosion resistance, but protection is not

complete, primarily because of discontinuities in the oxide. Greater corrosion resistance may be imparted to aluminum by increasing the thickness of the aluminum oxide film, as in the anodizing process. Anodizing does not, however, increase corrosion resistance in direct proportion to the increase in oxide thickness because of the porous nature of the film formed. Another method of increasing oxide thickness is through chemical reactions similar to chromate conversion coatings that form an oxide layer at an aluminum surface. Coatings of this type are based on the fact that Cr_2O_3 is both an insoluble oxide and forms a solid solution with Al_2O_3. Therefore a thicker, well-bonded film is easily formed on aluminum. Chromate coatings provide an example of a multicomponent oxide system.

C. MIXED OXIDE SYSTEMS: NEW TYPES OF PROTECTIVE COATINGS

In our original research proposal, it was stated that mixed oxide systems, i.e., distinct surface compounds formed from oxides in definite proportions, offer considerable promise for corrosion protection. Mixed oxide systems are perhaps best approached through a discussion of the acid-base characteristics of oxides, and we digress briefly to discuss this subject. In the general Lewis concept of acids and bases, a base is any substance capable of acting as an electron donor, and an acid is any substance capable of acting as an electron acceptor. The acid-base characteristics of a number of oxides of interest are summarized in Table 1. Oxides of nonmetals, e.g., NO_2, SO_3, are strongly acidic. Oxides of metals range from strongly basic, e.g., alkali metal oxides, to strongly acidic, e.g., CrO_3, Mn_2O_7. Several oxides are capable of displaying both basic or acidic character. Such oxides are called amphoteric.

The acid-base nature of an oxide is found to correlate reasonably well with the calculated charge on the oxygen, as is also indicated in Table 1. The calculated charge on oxygen reflects the electronegativity difference between oxygen and the cation. There are a variety of schemes for calculating charges on atoms in compounds based on different electronegativity scales. The oxygen charges in Table 1 have been computed by using the system of Sanderson (Ref. 9). Partial charges computed in this way are smaller in magnitude than those computed by using Pauling electronegativities; however,

Table 1. Partial Charge on Oxygen and Acid-Base Properties[a] of Oxides[b]

δ_o(units of /e/)	Oxide	Base	Acid
-0.96	Cs_2O	S	0
-0.57	CaO	S	0
-0.56	La_2O_3	S	0
-0.53	TiO	S	0
-0.45	Ti_2O_3	W	0
-0.42	MgO	W	0
-0.41	MnO	W	0
-0.40	NiO	VW	0
-0.40	CoO	$\overline{VW}$	VW
-0.40	FeO	$\overline{VW}$	VW
-0.39	Ta_2O_5	VW	$\overline{VW}$
-0.39	TiO_2	VW	$\overline{VW}$
-0.37	Cr_2O_3	$\overline{VW}$	VW
-0.35	MoO_2	0	0
-0.34	Mn_2O_3	VW	0
-0.33	Fe_2O_3	$\overline{VW}$	VW
-0.32	CuO	$\overline{VW}$	VW
-0.31	Al_2O_3	VW	VW
-0.31	WO_3	0	W
-0.29	MnO_2	VW	$\overline{VW}$
-0.28	MoO_3	0	M
-0.25	CrO_3	0	S
-0.20	Mn_2O_7	0	S
-0.08	SO_3	0	S
-0.05	NO_2	0	S

[a]S, strong; M, medium; W, weak; VW, very weak; $\overline{VW}$, very weak favored.
[b]Data taken from R. T. Sanderson, Inorganic Chemistry, Reinhold, New York (1967).

the numerical values obtained have considerable experimental justification, and the calculations may be readily performed for complex compounds. In any event, the details of the present discussion actually depend on the relative values of calculated charges, and this relative ordering does not critically depend on the method of calculation used.

The relevant observation pertinent to corrosion protection is that strongly acidic oxides will dissolve in basic and neutral media, whereas basic oxides will dissolve in acidic and neutral media. However, amphoteric oxides, although sparingly soluble in both strongly acidic and strongly basic media, are not soluble in the middle ranges of pH values important for corrosion protection of metal aircraft surfaces. In Table 1, it is shown that oxides such as Al_2O_3 and Cr_2O_3, which are generally thought of as protective, are in fact amphoteric, as would be expected.

We now note that three of the four criteria for corrosion protection set forth above may be inferred from Table 1. We have just discussed oxide solubility. The most basic oxides are known to be ionic conductors, hence unsuited as protective coatings from this standpoint as well as because of their solubility. On the other hand, the higher oxides of a metal tend to be less ionic than the lower oxides since more oxygen atoms are in competition for the electrons of the cation; hence the average oxygen partial charge is lowered. This effect is synonymous with higher acidity. Greater acidity is associated not only with increased solubility in aqueous neutral and basic media, but with increased electronic conductivity as well. Therefore, the criteria formulated in Section III.A also lead to the conclusion that amphoteric oxides provide the best choice for corrosion-resistant oxides.

By using mixed oxide systems for corrosion protection, the use of a whole new range of amphoteric complex oxides as protective films is opened for investigation. Furthermore, we devised a set of guidelines for the selection of candidate materials. Partial oxygen charges on several mixed oxides, calculated by using the methods of Ref. 9, are presented in Table 2. The charge on oxygen is intermediate between the oxygen charges in the constituent materials. In other words, the oxygen charge is amenable to manipulation to

Table 2. Enthalpy of Formation and Partial Charge on Oxygen in Some Mixed Oxide Systems

Compound	Partial Oxygen Charge δ (units of %e/)	ΔHf°(except) (kcal/mole)	ΣΔHf° of Component Oxides (kcal/mole)	ΔHf°(except) of Component Oxides − ΣΔHf° (kcal/mole)
CaO	-0.57	-151.79		
Ta_2O_5	-0.37	-489.0		
Al_2O_3	-0.31	-400.5		
$CaO.Al_2O_3$	-0.40	-556.0	-552.3	-3.71
$CaO.2Al_2O_3$	-0.36	-950.7	-952.8	+2.1
$2\ CaO.Al_2O_3$	-0.44	-707	-704.1	-2.9
$3\ CaO.Al_2O_3$	-0.46	-857.5	-855.9	-1.6
$4\ CaO.Al_2O_3$	-0.48	-1008	-1007.7	-0.3
$12\ CaO.7Al_2O_3$	-0.43	-4644	-4625	-19.0
$Ta_2O_5.Al_2O_3$	-0.35			

provide optimum corrosion protection. Since proper coordination with the substrate material is essential for corrosion protection, protective oxides are also required to have certain crystal structures with a certain range of lattice parameters. However, because of the large number of potentially useful oxide systems, it is in principle possible to simultaneously satisfy all necessary requirements and thus devise oxide films for aircraft aluminum alloys with truly superior corrosion resistance.

IV. FORMATION AND CHARACTERIZATION OF CHROMATE COATINGS

Although chromate conversion coatings have been used on aluminum since 1915 (Ref. 10), precisely how the chromate conversion reaction proceeds, the nature of the resultant protective coating, and the mechanism of corrosion protection were still not well understood prior to this investigation.

A. COATING DEPOSITION

1. EXPERIMENTAL PROCEDURES

All chromate coating solutions contain chromic acid or one of its soluble salts as a source of hexavalent chromium. However, no chemical reaction with the metal surface is observed unless other chemical species are added to the chromate solution in order to activate or promote the reactions that result in the formation of the coating. Coatings are usually applied to aluminum with one of many commercially available proprietary solutions. However, it was believed that, in order to study the mechanism of film growth, the exact chemical composition of the chromating solution had to be known. Therefore, the solutions were prepared by following various published formulas. Both the chemical composition and the concentration of solution constituents could then be varied in order to determine the effects on the composition and properties of the coatings. A coating produced from one of the commercially available solutions was also examined to make the study more relevant to current technology. Some recent studies have also characterized these coatings by surface methods (Refs. 11-15).

All coatings were applied to coupons of aluminum 1100 alloy (commercially pure 99.9% aluminum). Pure aluminum was selected in preference to the high-strength aluminum alloys to minimize the complicating effects of the alloying metals and to gain better insight into the reaction of aluminum with the various solutions. The procedure for preparing all coatings follows:

a. Degrease with trichloroethane in an ultrasonic bath at room temperature for 2 to 5 min.

b. Rinse with distilled water.

c. Clean in an alkaline solution consisting of 18 g/liter Na_2CO_3 and 8 g/liter Na_2SiO_3 at 90°C for 4 to 6 min.

d. Rinse with distilled water.

e. Clean with Alumiprep (Amchem Products), which contains phosphoric acid and a detergent, at room temperature for 4 to 6 min.

f. Rinse with distilled water.

g. Immerse in chromate conversion coating solution.

h. Rinse with distilled water.

i. Dry in air at 55 to 60°C for 15 to 20 min.

j. Store in a dessicator.

All coatings were analyzed for their surface elemental composition using AES. Specimens were then depth profiled (see Section II).

The energies of the Auger peaks simultaneously monitored during depth profiling were: oxygen, 503 eV; aluminum, 1378 eV; chromium, 571 eV; and fluorine, 647 eV. The approximate sputter rate was determined at 8×10^{-5} Torr argon pressure, 2-kV accelerating voltage, and 20-mA ion beam current, to be 100 ± 15 Å/min for Ta_2O_5. The coating thickness is taken as the depth at which the oxygen signal decreases to 10% of the surface value. Since the coating thickness for each treatment varies slightly from coupon to coupon, as well as from site to site on the same coupon, the thickness values presented are the average of at least six sites on at least three similarly prepared coupons. The standard deviation is reported where appropriate. Since the sputter rate for Ta_2O_5 may differ from that for CrOOH or AlOOH (Ref. 16), the absolute values of the depths reported here must be considered approximate. However, the depths were measured consistently, and the relative depth values are more accurate than the absolute values.

The relative amounts of chromium (III) and chromium (VI) on the surfaces of the various coatings were determined by XPS analysis. The overlapping chromium $2P_{3/2}$ peaks were resolved by fitting two Gaussian curves to the spectra. Ion microprobe mass analysis (more sensitive than Auger spectroscopy for some species) revealed no cations other than chromium and aluminum in any of the coatings studied.

Salt fog corrosion-resistance evaluation was conducted as described in Section II.

It was determined that in order for a corrosion-resistant coating to form on aluminum, either hydrogen fluoride or hydroxide ions must be present in the coating solution in combination with the hexavalent chromium. The two simplest coating formulas that typify this combination are the alkaline modified Bauer-Vogel (MBV) solution (Ref. 17) and the acidic Standard Telephones and Cables (STC) solution (Ref. 18). The MBV coating solution consists of 30 g/liter Na_2CO_3 and 15 g/liter Na_2CrO_4. The carbonate hydrolyzes in solution and results in a pH of about 11. This coating is applied by immersion in the solution for 3 to 4 min at 90°C. The STC solution contains 4 g/liter CrO_3, 3 g/liter $Na_2Cr_2O_7 \cdot 2H_2O$, and 0.8 g/liter NaF. It is applied at 30°C for 3 to 4 min. The predominant fluoride species at this fluoride concentration (approximately 2×10^{-2}M) and pH (approximately 1.5) is HF (Ref. 19).

The mechanisms of film growth of the MBV and STC coatings are probably similar, with the hydroxide ions and the hydrogen fluoride playing analogous roles. However, since many of the currently used proprietary solutions have the chromate-fluoride formula as a basis (Refs. 11, 12), the emphasis in this study is on the STC coating solution.

2. COATING CHARACTERIZATION

The modifications of the STC solution studied include variations in the chromate, fluoride, and hydrogen ion concentrations, as well as the solution temperature and time of immersion of the aluminum coupons. Auger depth profiles of the coatings resulting from each of these variations were correlated with the corrosion resistance demonstrated in the salt-fog chamber. The results are summarized in Table 3.

An Auger depth profile of aluminum after cleaning with "Alumiprep" and rinsing with distilled water is shown in Fig. 1. A thin aluminum oxide layer covers the metal (60 to 80 Å thick). No residue from either the phosphoric

Table 3. Corrosion Resistance and Film Thicknesses

Procedure	Time to Visible Corrosion in Salt-Fog Chamber (hr)	Thickness (Å)
After cleaning with Alumiprep	5 - 10	60 ± 20
STC coating, 30 sec to 16 min in solution, 30°C, pH = 1.5	200 - 250	700 ± 100
MBV coating	225 - 275	3000 ± 500
Alodine 1500 coating	175 - 225	1000 ± 200
STC coating without NaF	10 - 20	160 ± 20
STC coating, 5 sec in solution	50 - 75	175 ± 40
STC coating, 10 sec in solution	70 - 90	300 ± 30
STC coating, 15 sec in solution	60 - 80	365 ± 35
STC solution, 5 sec followed by 4 min in STC without NaF	45 - 60	100 ± 20
STC solution, pH = 1.1	200 - 250	640 ± 100
STC solution, pH = 2.0	200 - 250	675 ± 100
STC solution, pH = 2.5	150 - 200	400 ± 50
STC solution, pH = 3.5	80 - 120	280 ± 50
STC solution, pH = 4.8	25 - 50	200 ± 50
STC solution, NaF × 0.1	25 - 35	200 ± 50
STC solution, NaF × 10	25 - 35	170 ± 50
STC solution, NaF × 0.5	200 - 250	740 ± 70
STC solution, NaF × 2	210 - 270	710 ± 70

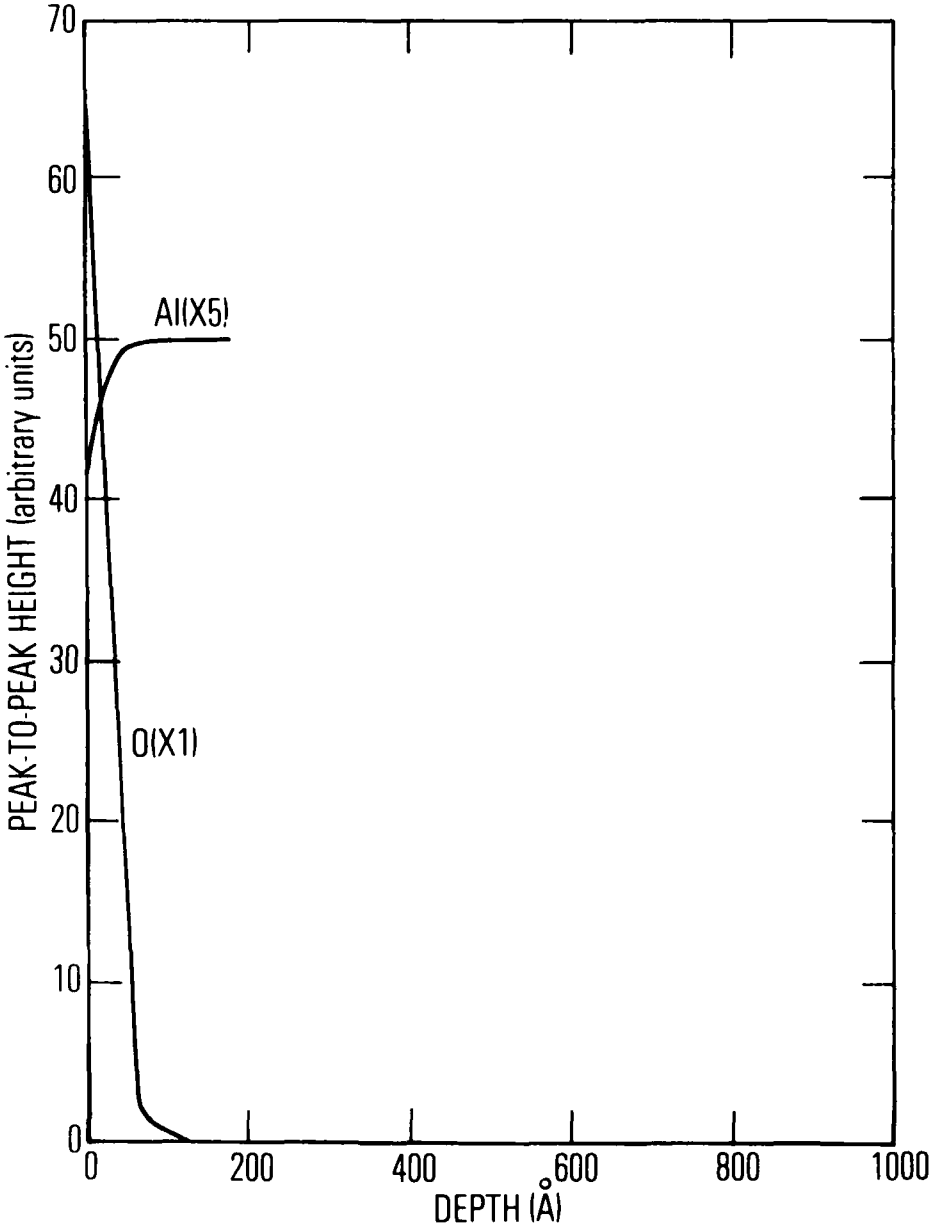

Fig. 1. Samples After Cleaning with Alumiprep

acid or the detergent is detected on the surface. This natural oxide coating offers very little protection from corrosion in the salt-fog chamber (Table 3). Figure 2 is a depth profile of the STC coating, which is about 700 Å thick and consists of a layer of chromium oxide over a layer of mixed chromium-aluminum oxide. Very little aluminum was detected on the surface. A small amount of fluoride was found throughout the coating, and a small amount of sodium (<1%) was detected on the surface of some samples. However, no sodium was detected in any sample at depths greater than 10 Å. This lack of sodium in the coating was confirmed with IMMA, by which as little as 10 ppm sodium can be detected. The approximate surface concentrations of the elements found are: oxygen, 63 at%; chromium, 31 at%; fluorine, 3 at%; and aluminum, 3 at%. The chromium is found throughout the coating, extending to the interface between the aluminum metal and the oxide. After the chromium is at a maximum of approximately 120 Å, the oxygen-chromium atomic ratio is about 1.8:1 and is constant throughout the coating to the aluminum metal surface. X-ray photoelectron spectroscopy data on these samples indicate that both trivalent and hexavalent chromium are present on the surface in the approximate ratio of 2:1 [Cr(III):Cr(VI)]. The crystalline structure cannot be detected in the coating by electron means or x-ray diffraction, indicating that it probably is amorphous.

The Auger depth profile of the MBV coating is very similar to that of the STC coating except that no fluorine is present and the thickness is approximately 3000 Å. A commercial chromate-fluoride coating known as Alodine 1500 (Amchem Products) also has a similar depth profile to that of the STC and a thickness of approximately 1000 Å. No coating is formed when NaF is omitted from the STC solution or when it is replaced by equal molar quantities of NaCl or Na_2SO_4. A depth profile of the coating resulting with the NaF omitted from the STC solution is shown in Fig. 3. In this case, the chromium does not penetrate to the aluminum-oxide interface, but is located on top of the aluminum oxide layer.

Neither the thickness nor the corrosion protection of the STC coating varies with the amount of time the coupon is immersed in the solution (30 sec to 16 min) (Fig. 4). However, the amount of aluminum in the solution, as

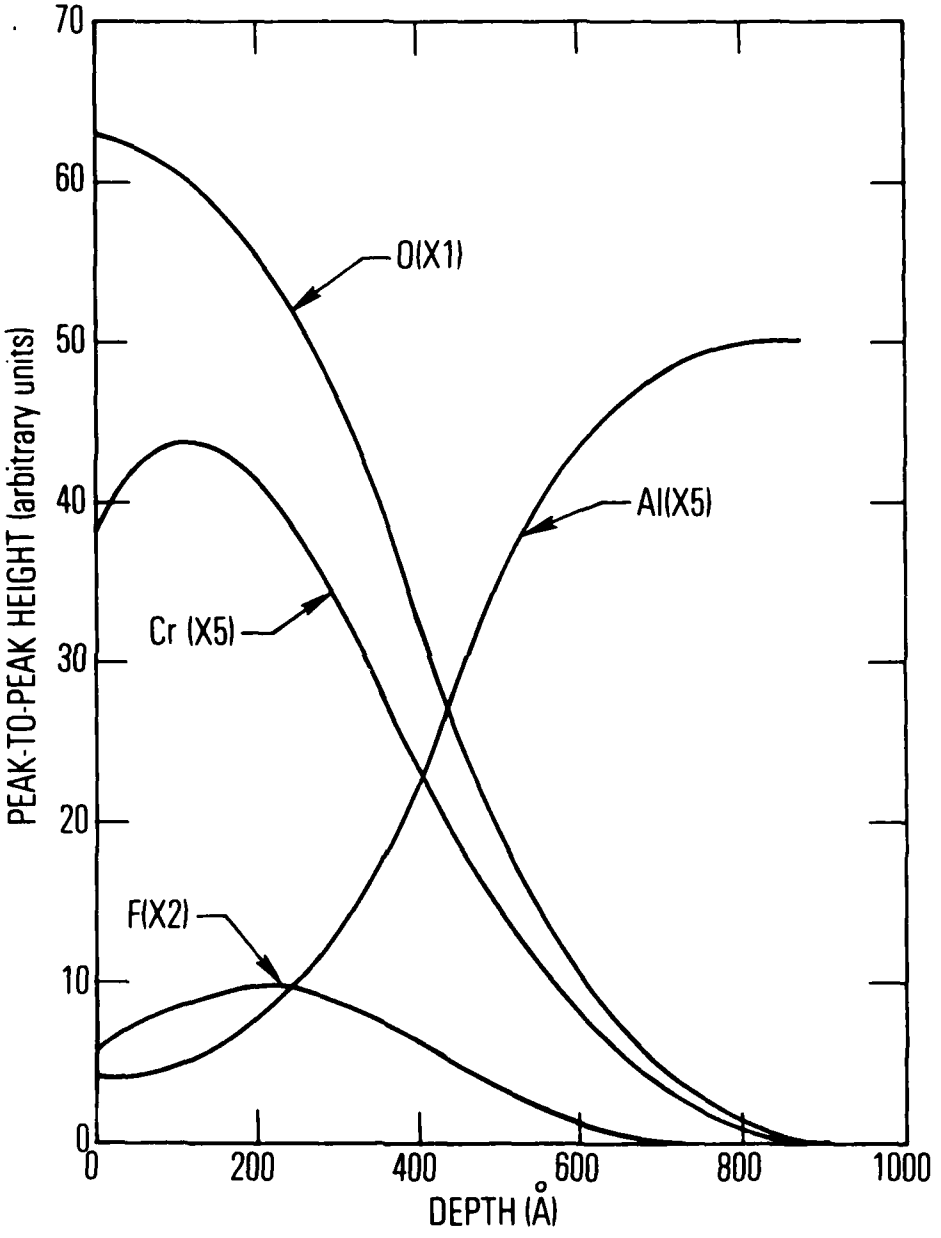

Fig. 2. STC Coating at 30°C

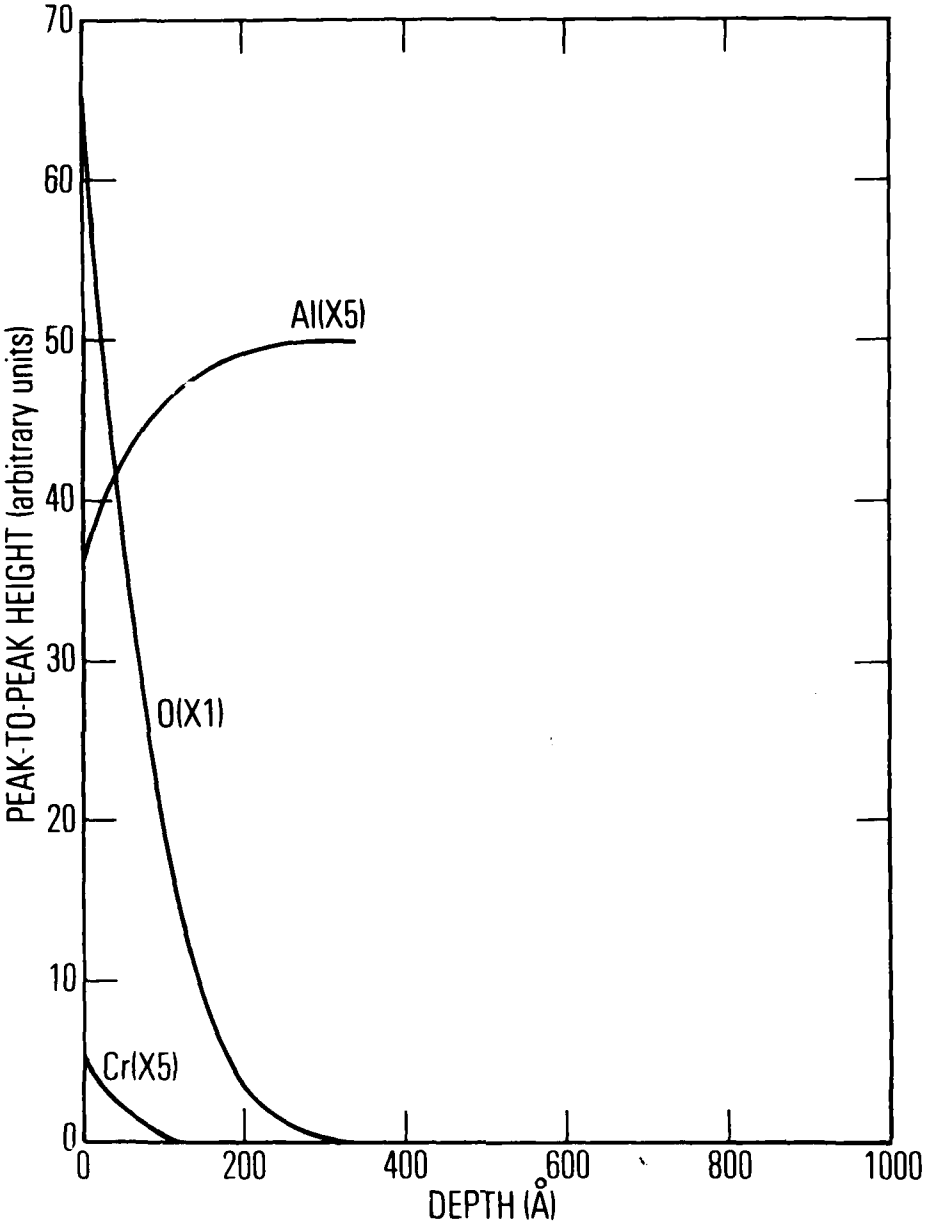

Fig. 3. Coating After 4 min in STC Solution with NaF Omitted

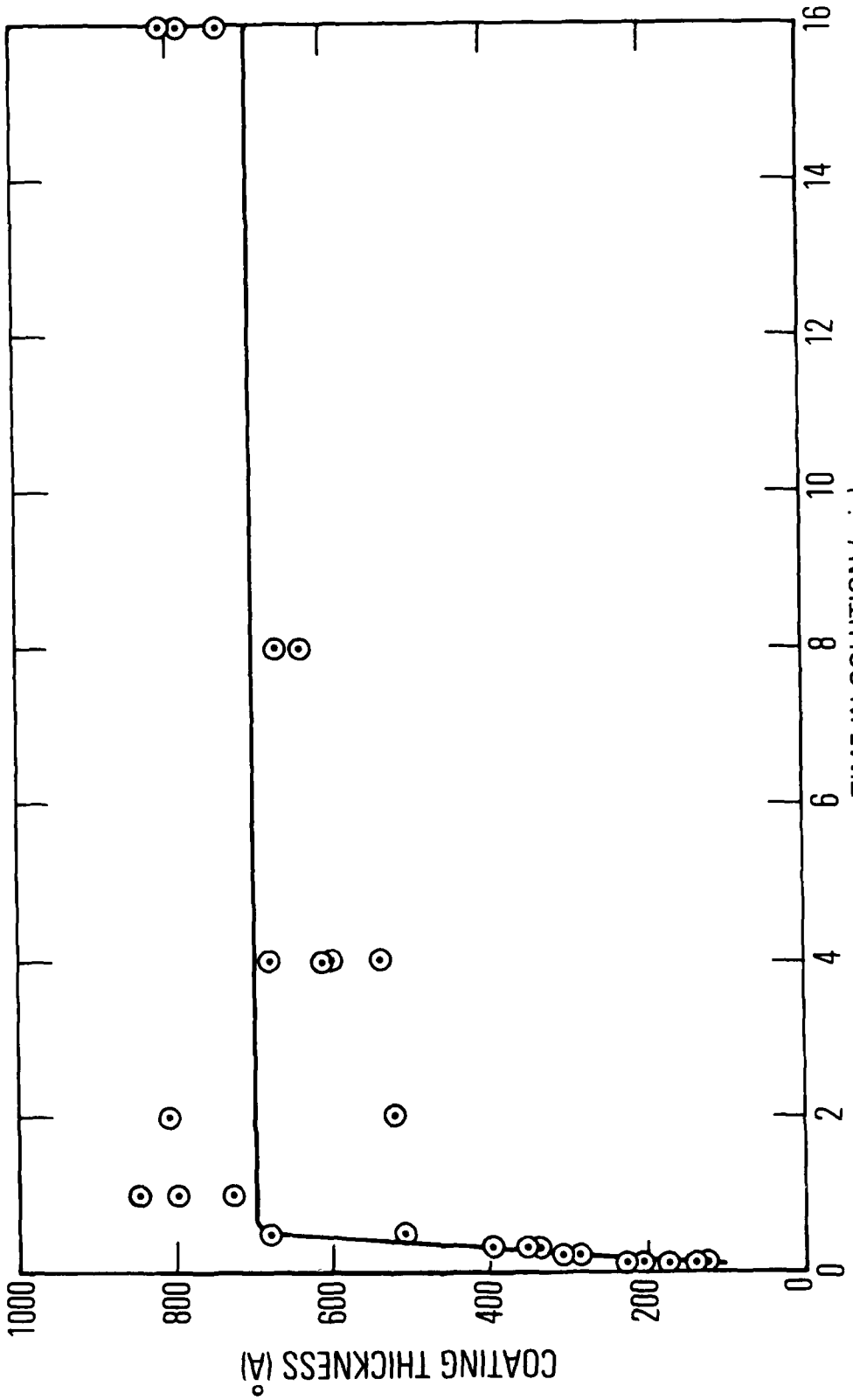

Fig. 4. STC Coating Thickness vs Time in Solution

determined by atomic absorption spectroscopy, increases with time (Fig. 5). The coating thickness varies with the temperature of the solution (25 to 40°C). The coating is thicker at the lower temperatures, and the variation is about -15 Å/°C (Fig. 6). However, no variation in corrosion protection was observed in any of the samples prepared in this temperature range.

The pH of the STC solution varied from approximately 1.1 to 4.8 by changing the CrO_3:$Na_2Cr_2O_7 \cdot 2H_2O$ ratio while holding the total amount of Cr(VI) constant. The coating thickness and corrosion protection are similar from pH 1 to approximately pH 2, but at higher pH the coatings produced are thinner (Fig. 7) and less corrosion resistant (Table 3). The F^- or Cr(VI) concentrations can be varied by a factor of two in either direction without affecting the thickness or corrosion protection. However, varying the F^- concentration by a factor of ten in either direction results in a thin (100 to 150 Å) coating with very poor corrosion resistance (Table 3).

B. MECHANISM OF COATING GROWTH

The observation that only a very thin chromate film is formed on top of the aluminum oxide layer when the fluoride is omitted from the STC solution (Fig. 3) and that chromium is found at the metal-oxide interface in the STC coatings (Fig. 2) leads to the conclusion that, in order for film growth to proceed, the chromate solution must directly contact the aluminum metal. The initial aluminum oxide surface coating must be penetrated in order for contact to occur, which is probably one reason why hydrogen fluoride or hydroxide is necessary in the coating solution. Aluminum oxide is etched in either a hydrogen fluoride solution at pH 1.5 (Ref. 15) or a hydroxide solution at pH 11 (Ref. 10):

$$AlOOH + 3\ HF \rightarrow AlF_3\ (soluble) + 2H_2O \qquad (1a)$$

$$AlOOH + OH^- + H_2O \rightarrow Al(OH)_4^-\ (soluble) \qquad (1b)$$

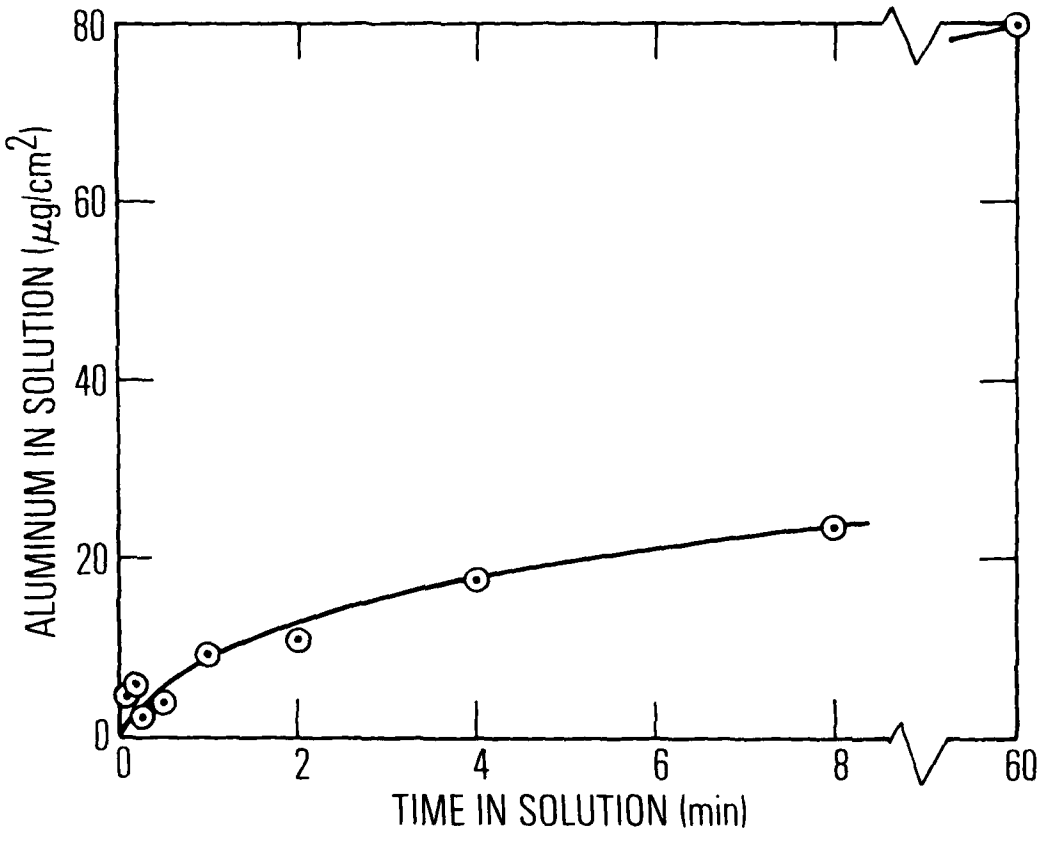

Fig. 5. Aluminum Dissolved in STC Solution at 30°C

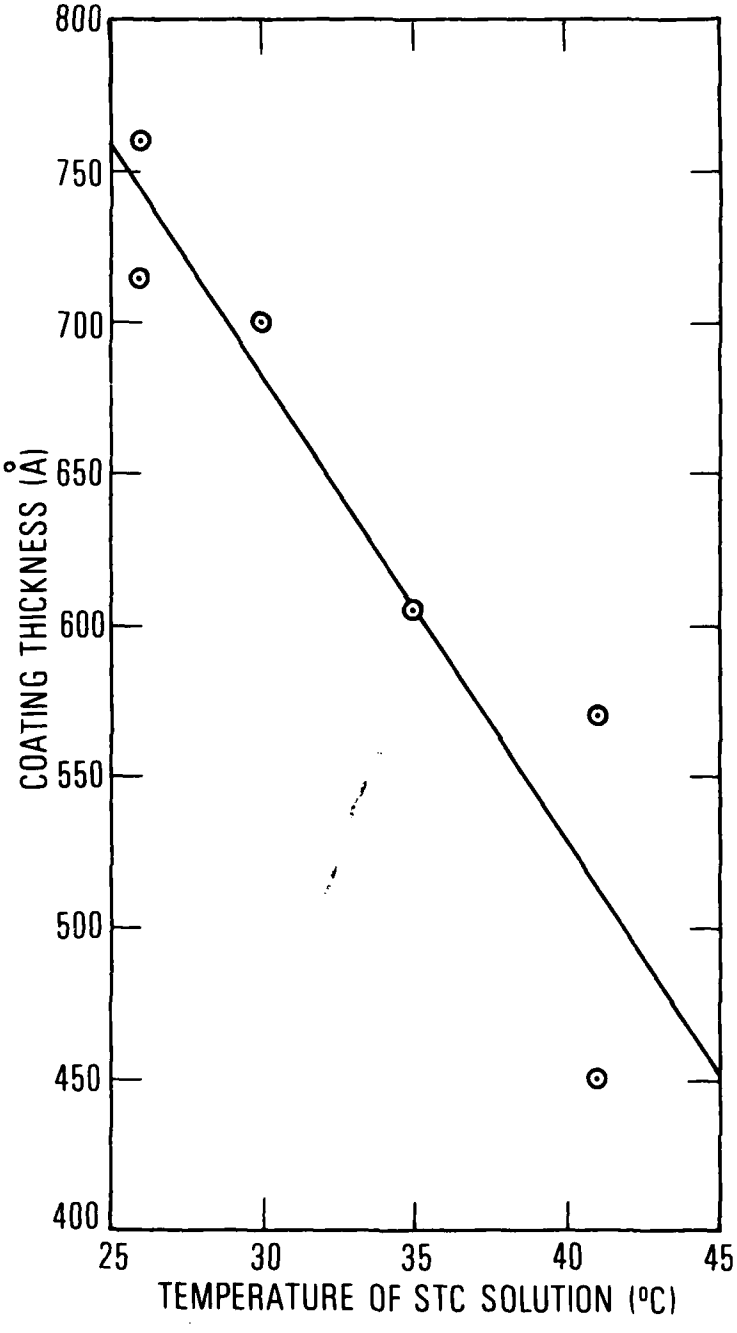

Fig. 6. Coating Thickness vs Temperature of STC Solution

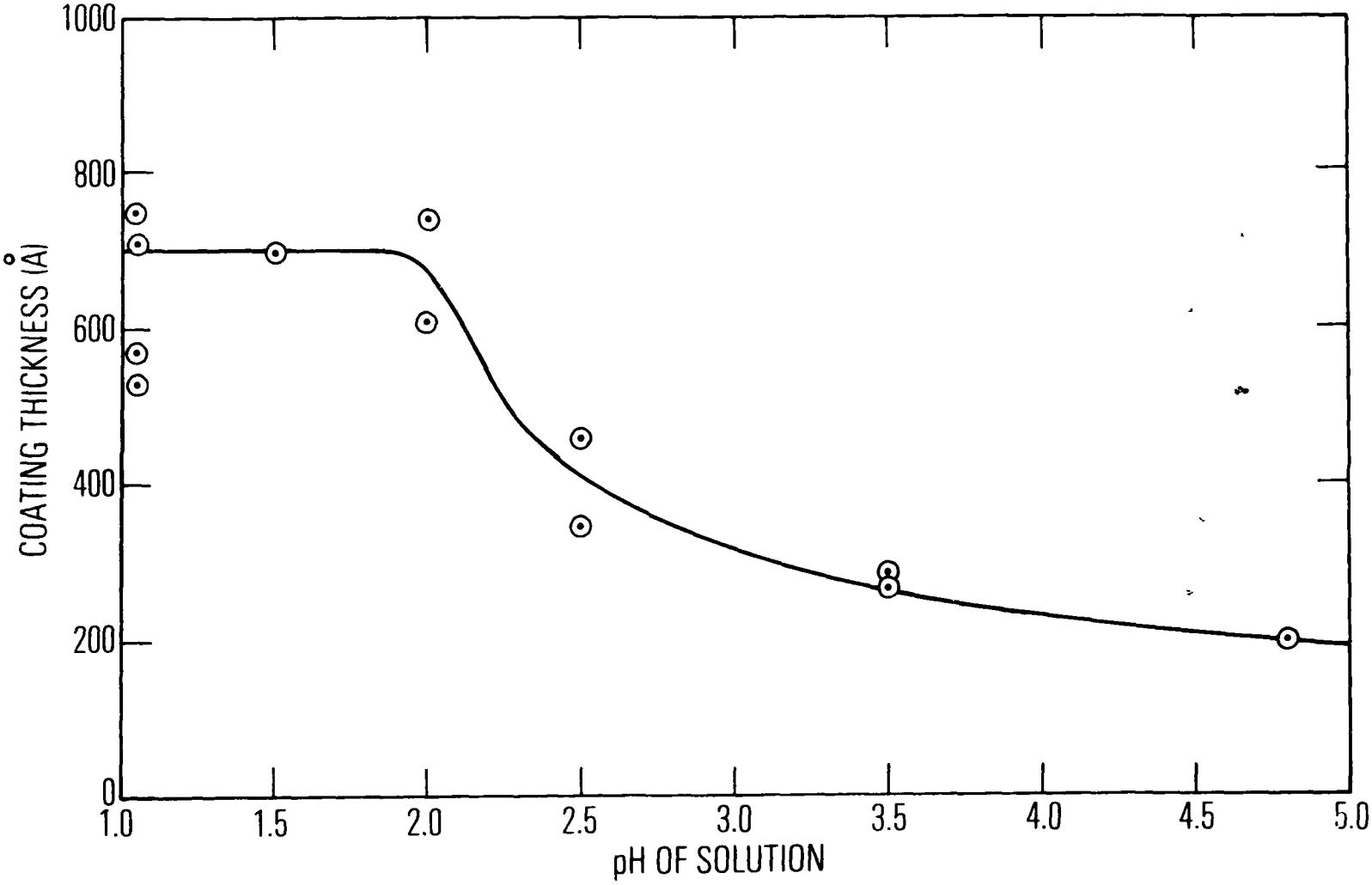

Fig. 7. Coating Thickness vs pH of STC Solution

In addition to their role in the initial dissolution of aluminum oxide, the fluoride or hydroxide ions play a role throughout the coating growth process. Aluminum coupons were immersed in the STC solution for 5 sec and then quickly transferred without rinsing to a solution containing identical concentrations of CrO_3 and $Na_2Cr_2O_7$, but no NaF, for 4 min. Five seconds in the STC bath was sufficient time to etch the original oxide film and for the STC coating to start growing (Fig. 8). If the hydrogen fluoride served only this purpose, then the coating on the coupon described would be the normal STC coating. However, a much thinner coating with very poor corrosion resistance results from this treatment (Fig. 9), indicating that the hydrogen fluoride plays a continuing role in the coating growth process.

After the protective aluminum oxide coating is etched by the hydrogen fluoride, the next reaction in the postulated mechanism is the reaction of the dichromate with the aluminum metal:

$$Cr_2O_7^{=} + 2Al^{\circ} + 2H^{+} + H_2O \rightarrow 2CrOOH\downarrow + 2AlOOH\downarrow \qquad (2)$$

The precipitation of the hydrated mixed oxide on the aluminum metal surface begins the coating growth. The AlOOH in the mixed oxide is then dissolved by the hydrogen fluoride, leaving the less soluble CrOOH on the surface. This process continues as the coating grows outward from the metal surface. Aluminum metal or oxide is dissolved wherever it contacts the solution and is replaced with insoluble amorphous hydrated chromium (III) oxide, which protects the aluminum from further attack by the hydrogen fluoride. The solution continues to attack through any weak spots in the coating, and any channel that would otherwise be available for a corroding ion to penetrate becomes clogged with impervious hydrated chromium oxide:

$$2Al^{\circ} + Cr_2O_7^{=} + 2H^{+} + 6HF \rightarrow 2AlF_3(\text{soluble}) + 2CrOOH\downarrow + 3H_2O \qquad (3).$$

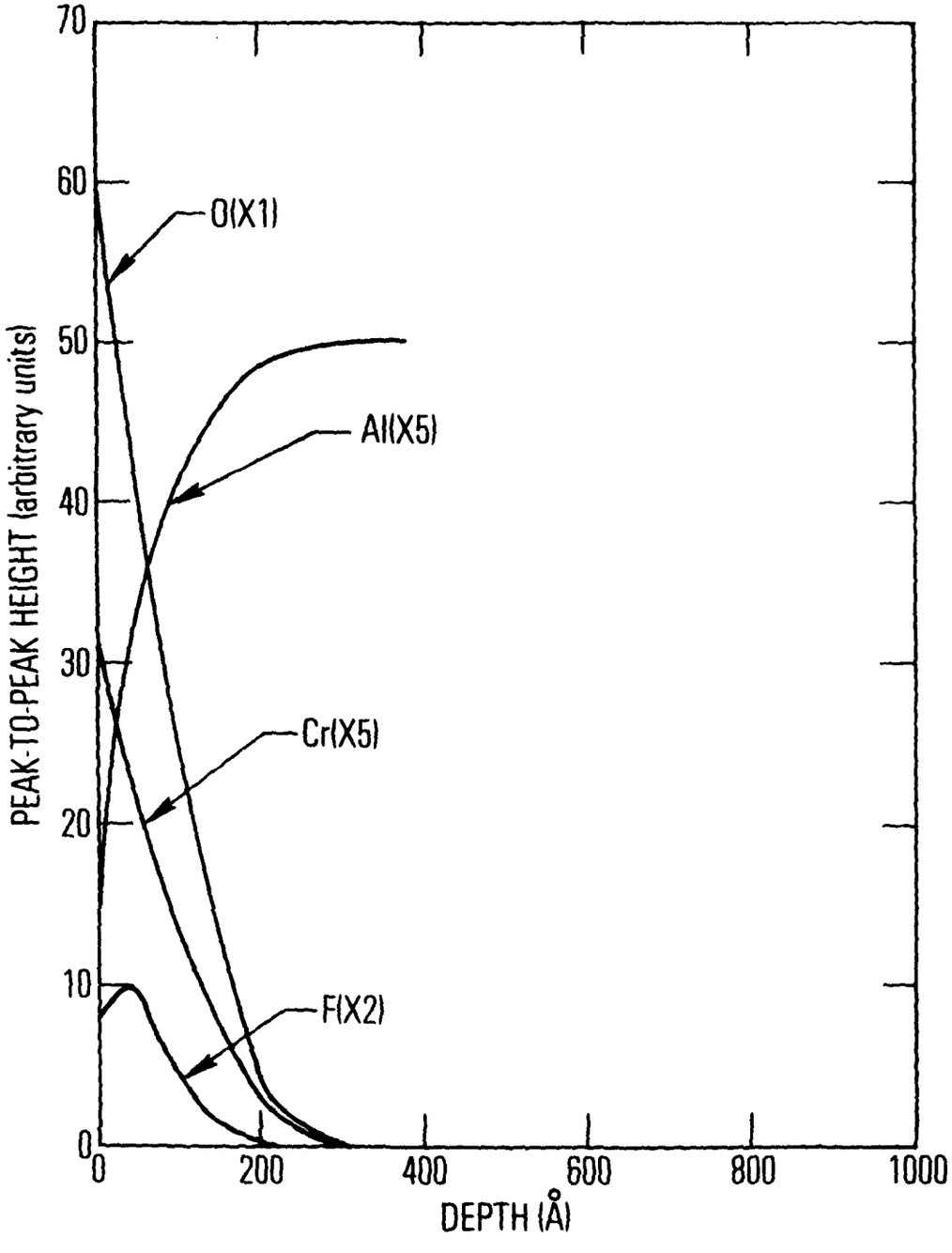

Fig. 8. Coating After 5 sec in STC Solution

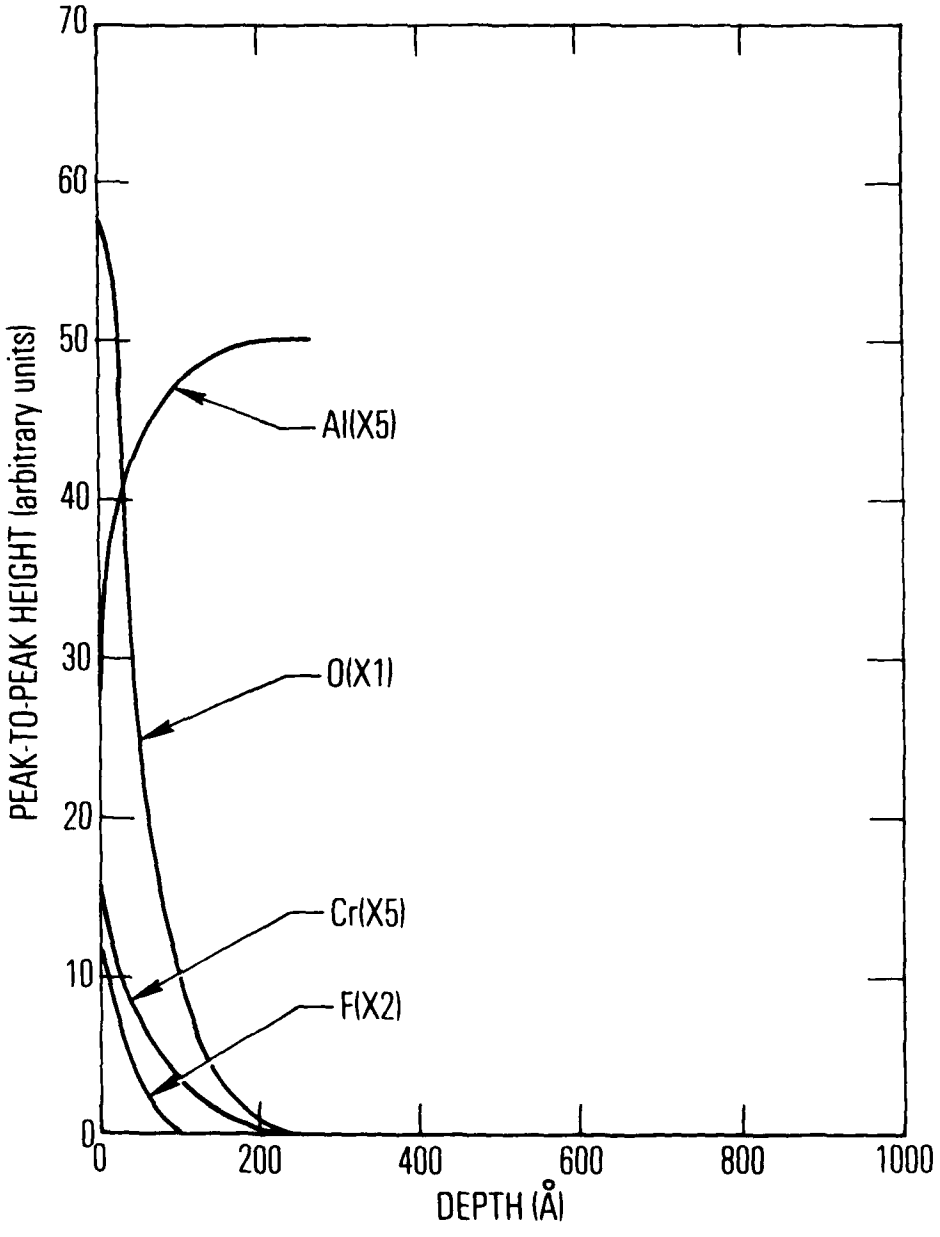

Fig. 9. STC Solution for 5 sec Followed by 4 min in STC Solution with NaF Omitted

Some of these weak spots and channels may be created by the fluoride ions that are incorporated into the coating.

As the coating continues to grow, it is probable that more aluminum metal is oxidized at the metal-oxide interface as electrons are drawn through the coating by the oxidizing action of the chromate ions adsorbed on the surface. Since any Al^{+3} ion that travels through the coating to the surface is dissolved into the solution, a concentration gradient develops, and a dynamic equilibrium is established between aluminum oxidation at the metal-oxide interface and Al^{+3} dissolution at the surface. This process is shown schematically in Fig. 10. The aluminum metal is oxidized to Al^{+3} at the metal-oxide interface, and the Al^{+3} ions diffuse through the coating to the surface, where they are dissolved into the solution. Data shown in Fig. 5 indicate that at 30°C, steady state, the aluminum dissolves at the rate of about 1 $\mu g/cm^2/min \cong 40$ Å of Al/min. The electrons are drawn through the coating, reducing the $Cr_2O_7^{=}$ adsorbed on the surface.

The CrOOH that is deposited on the surface is somewhat soluble in the STC solution:

$$CrOOH + 3\ HF \rightarrow CrF_3(\text{soluble}) + 2H_2O \qquad (4)$$

which indicates that the coating surface is continuously dissolving and reforming. The steady-state equation after the coating reaches equilibrium thickness is postulated to be the sum of Eqs. (4 and 5):

$$2Al^\circ + Cr_2O_7^{=} + 2H^+ + 12HF \rightarrow 2AlF_3 + 2CrF_3 + 7H_2O \qquad (5)$$

The net effect is the dissolution of aluminum metal with a concurrent buildup of trivalent chromium in the solution. The expected rise in the pH of the solution as the H^+ is depleted with time was observed.

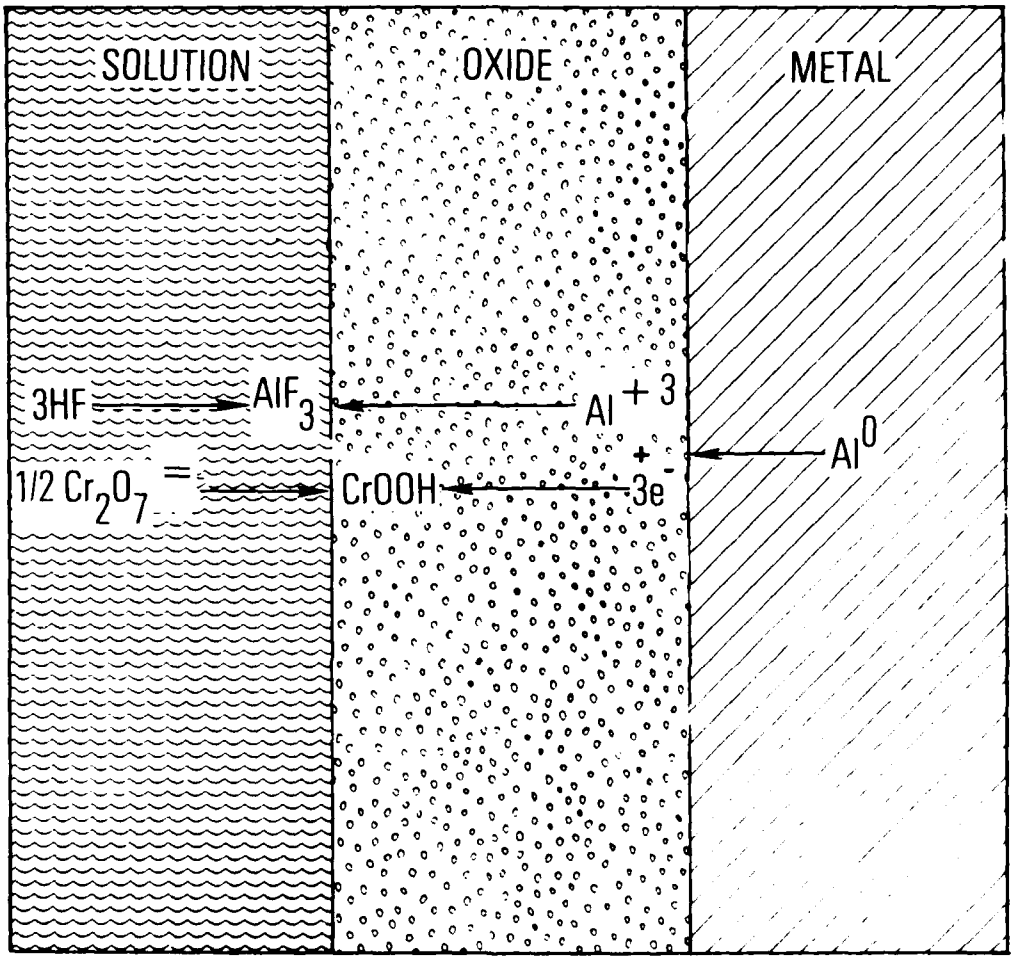

Fig. 10. Mechanism of Coating Growth

Since the coating thickness does not continue to increase with immersion time after 30 sec, one of the reactions in the mechanism described previously must limit the equilibrium thickness. One possibility is that the coating thickens until the metal is screened from the oxidizing potential of the solution. In this case, the electronic resistivity of the coating reaches a limiting value, and the oxidizing power of the chromate solution is no longer felt at the metal-oxide interface. Aluminum oxidation ceases until some of the coating is dissolved, at which time the resistivity drops, and oxidation begins again.

Another equally likely possibility is that, after the initial formation of the coating, the CrOOH being deposited on the surface dissolves at the same rate at which it is produced. The temperature dependence (Fig. 6) suggests that, at higher temperatures, the rate of Eq. (4) (CrOOH dissolution) may be increased more than the rate of Eq. (3) (CrOOH formation). Therefore, the kinetic equilibrium between coating formation and coating dissolution is shifted slightly toward dissolution, and the coatings are thinner at the higher temperatures. However, the effect may also be explained if it is assumed that the equilibrium of Eq. (4) is shifted to the right at higher temperature and the equilibrium of Eq. (3) is less temperature dependent. In either case, the dissolution of CrOOH can act as the thickness-limiting reaction. The CrOOH dissolution mechanism is consistent with the fact that the MBV coatings are thicker than the STC coatings because CrOOH is less soluble in the alkaline MBV solution than in the acidic STC solution (Ref. 19).

The growth mechanism described is consistent with the depth profile data for the coatings at various stages in their growth. A depth profile of the coating after 5 sec in the STC solution is shown in Fig. 8, and the profiles after 10 and 15 sec are shown in Figs. 11 and 12, respectively. After 5 sec, the original AlOOH coating is breached, and the chromate starts to attack the aluminum (chromium is found at the metal-oxide interface). At this point, the coating is approximately 200 Å thick. By means of XPS the chromium on the surface is revealed to be mainly trivalent, but a small fraction (< 10%) is hexavalent. After 10 sec in the solution, the chromium on the surface has reached its equilibrium value (approximately 31%), and a concentration maximum

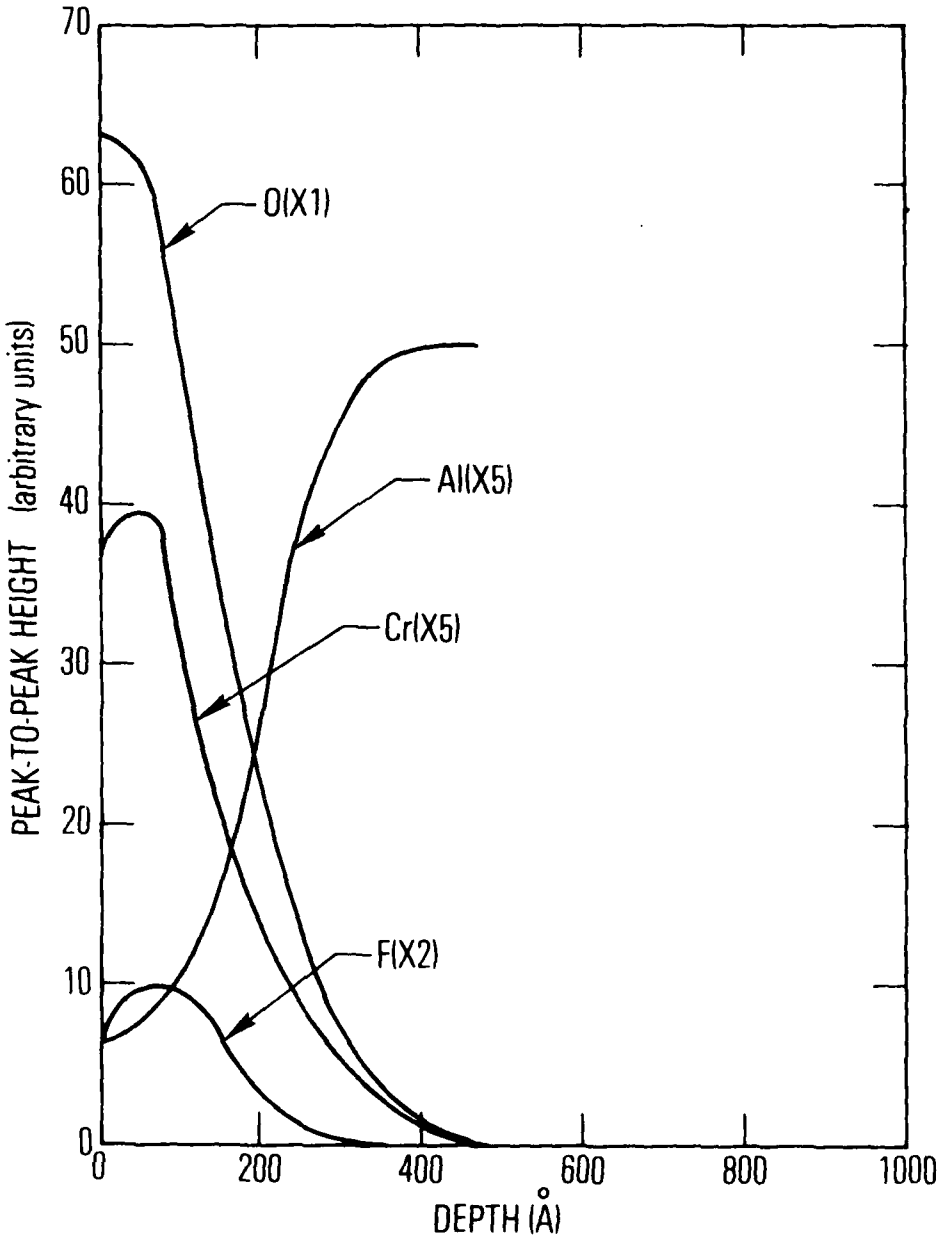

Fig. 11. Coating After 10 sec in STC Solution

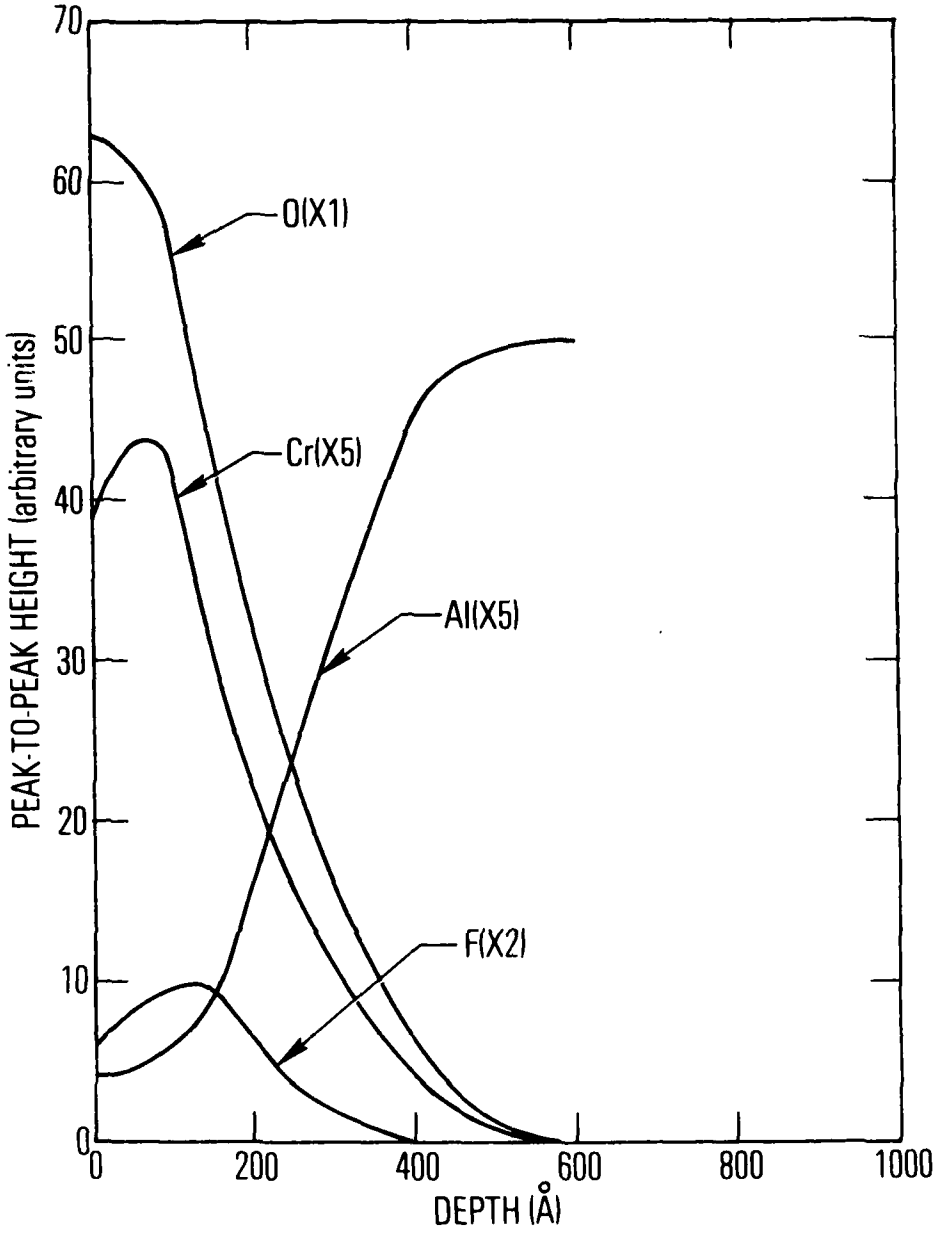

Fig. 12. Coating After 15 sec in STC Solution

starts to form. At this point, the coating is approximately 300 Å thick. After 15 sec, the depth profile indicates that qualitatively the coating is completely formed, but it is only about 400 Å thick. After 30 sec, the coating is completely formed (approximately 700 Å thick, Fig. 2). It appears that some chromate ions remain strongly adsorbed on the surface and are found in decreasing quantities within 120 Å of the surface. The oxygen-chromium ratio is higher in chromate, which explains why the ratio is greater on the surface and gradually decreases with depth to the chromium maximum at 120 Å. Between this depth and the metal-oxide interface, the chromium is expected to be totally trivalent, which would explain the constant oxygen to chromium ratio that is observed.

A further role for the fluoride ions incorporated into the STC coating is suggested by Valand and Nilsson in a recent paper (Ref. 20). They found that both anodic and cathodic reaction rates were increased when F^- ions were introduced into the oxide layer on high-purity aluminum electrodes. They allowed the electrodes to stabilize in solutions of varying fluoride ion concentrations (5×10^{-5} to 10^{-2}M) at pH 5.25. After stabilization, varied potentiostatic steps of short duration were applied to the electrodes and the resultant current densities were measured. Their results indicate that both the anodic and cathodic reaction rates increase with increases in fluoride ion concentration. They explain this effect by assuming that the F^- ions replace some of the $O^=$ ions in the oxide since the ionic radii are similar (r_{F^-} = 1.36 Å and r_O = 1.40 Å). The change in charge distribution caused by this replacement increases both the ionic and electronic conductivity, which increases the rates of the electrode reactions. The ionic conductivity is increased more because of the formation of Al^{+3} vacancies in the lattice (fewer Al^{+3} are needed for charge neutrality in AlF_3 than in Al_2O_3). These cation vacancies increase the transport rate of the Al^{+3} through the oxide by means of a vacancy-hopping mechanism. In the STC coating, the fluoride ions that are incorporated into the oxide coating would be expected to increase the mobility of the Al^{+3} by a similar mechanism. In addition, it has been shown theoretically (Ref. 21) that ionic conduction by an impurity-induced mechanism is greatly enhanced in thin films near room temperature compared to intrinsic conductivity mechanisms.

The predominant fluoride species in the solution at pH 1.5 is hydrogen fluoride; at higher pH, its concentration is lowered as it dissociates:

$$HF \rightarrow H^+ + F^- \qquad (6)$$

where (HF) = (F^-) at pH 3.2 (Ref. 19), which may explain the dependence of the coating thickness on pH (Fig. 7). As the HF concentration decreases at higher pH, more aluminum and less chromium is found on the surface and throughout the coating, which is thinner and less corrosion resistant. At pH 4.8, the coating is only slightly thicker and more corrosion resistant than the coatings formed in the total absence of fluoride (Table 3).

V. TITANATE COATINGS

Our detailed study of the chromate coating system, largely completed during the first year of program effort, provided insight into the function of protective oxide coatings and provided a standard against which to measure the performance of new coating formulations.

Titanate-based oxide coatings were studied as a prototype system to establish the feasibility of depositing protective mixed oxide films on aluminum at room temperature under benign conditions. We wanted to examine a coating system using a nonoxidizing metal reactant (as opposed to highly oxidizing Cr^{+6}) in which oxygen from the air or dissolved in the solvent oxidizes aluminum. Neither HF nor OH^- is necessary to penetrate the initial surface oxide layer. Coating formation proceeds by a substitution reaction with the oxide. Other investigations have previously studied the mechanism of hydrolysis in solution (Refs. 22-30). The titanium alkoxides are readily available commercially (Dupont "Tyzor" Products).

A. EXPERIMENTAL PROCEDURES

In the initial phase of the investigation of the titanium-aluminum system, coatings were deposited on commercially pure (AA* 1100) or high-purity (99.999%) aluminum. After developing a mechanism for coating formation, the work was extended to encompass coating deposition on three of the most common structural aluminum alloys. The coating procedure is the same for all materials.

The experimental procedure for coating formation is divided into three parts: (a) preparation of aluminum surfaces that have thin reproducible layers of aluminum oxide; (b) application of a thin unconsolidated titanate film by immersion of the specimen in coating solution; and (c) hydrolysis and drying of the coating. Figure 13 is a flow chart illustrating these procedures.

*American Aluminum Association designation.

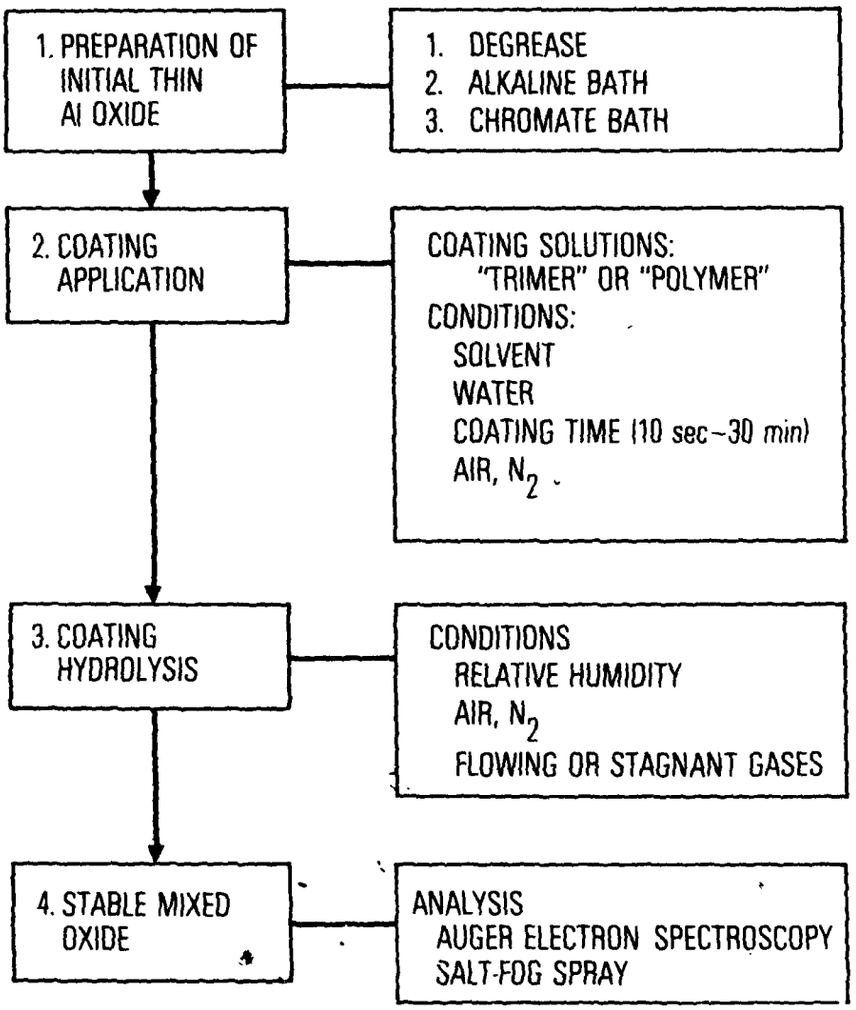

Fig. 13. Coating Steps and Analysis

For initial preparation, the test coupons were (Ref. 10): (a) degreased with trichloroethane in an ultrasonic bath at room temperature for 2 to 5 min; (b) cleaned with an alkaline solution that contained 18 g/liter Na_2CO_3 and 8 g/liter Na_2SiO_3 at 90°C for 4 to 6 min; (c) rinsed with distilled water; (d) cleaned with a chromate cleaning solution that contained 175 g/liter CrO_3 and 35 g/liter H_2SO_4 at 40 to 60°C for 4 to 5 min; (e) rinsed with distilled water; and (f) air dried overnight.

Aluminum coupons, hung on Teflon-covered wires, were immersed in the coating solution for time intervals of 10 sec to 30 min. Coatings were formed using several different types of organic titanates. Most of these titanates have the general formula $Ti(OR)_4$, where "R" represents an isopropyl group (Tyzor TPT), an n-butyl group (Tyzor TBT), or a 2-ethyl hexyl group (Tyzor TOT). A partially hydrolyzed Tyzor TBT (Tyzor PB) was also used as was an acetylacetonate chelate complex (Tyzor AA).

In the case of the titanium alkoxides, the rate of film formation depends on the length of the R group. Reaction rates with the tetrabutyl titanate were found to give the best performance, and Tyzor TBT was thus employed exclusively in our later investigations. Coating solutions consisted of 0.01 to 0.1 M Dupont Tyzor TBT in either reagent grade isopropanol or toluene. These solvents were dried at least 12 hr with anhydrous magnesium sulfate. Known amounts of water were added for experiments using wet solvents. In some experiments, solvents were purged with nitrogen before the titanate was added in order to test the effect of oxygen on coatings. TBT is normally present in solution as the trimer. More highly polymerized TBT was formed by the addition of water to trimeric TBT; 0.5 M TBT solutions in isopropanol were mixed with small amounts of water (0.02 to 0.1 M) and were aged at least 8 hr. The solutions were then diluted to 0.06 M TBT with isopropanol and applied to coupons. The partially polmerized commercial Tyzor product, Tyzor PB, was not sufficiently well characterized with respect to degree of polymerization for our purposes.

Hydrolysis of the coated aluminum coupons was effected by hanging the coupons in crystallizing dishes (15 cm in diameter) that were enclosed in polyethylene bags. A small dish of water was placed in the bag for 100% relative humidity, or a small dish of Drierite was placed in the bag for low (less than 10%) relative humidity. Either nitrogen or air could be flowed through the bag to study the effect of flowing gases on coating hydrolysis. Some coatings were hydrolyzed in room air at 30 to 100% relative humidity. All hydrolysis took place at room temperature.

Characterization of deposited titanate coatings, and the evaluation of coating corrosion resistance, were accomplished using the general methods discussed in Section II. In addition to the Auger peaks listed in Section IV.A.1, the titanium LMM peak at 380 eV was monitored in this phase of the study. Sputter rates under ion bonbardment were as discussed in Section IV.A.1. It was convenient to define the total coating thickness as the depth at which the oxygen or titanium signals dropped to 10% of the surface values, t(10%). The beginning of the mixed region is defined as the depth at which the oxygen or titanium signal dropped to 90% of the surface value, t(90%) (Fig. 14). The fraction of mixed oxide, f, in this coating is defined by:

$$f = [t(10\%) - t(90\%)]/t(10\%)$$

B. GENERAL MECHANISM OF FILM FORMATION

As stated in Section V.A, the formation of the corrosion-resistant titanium-aluminum oxide films is accomplished in two stages, application and hydrolysis steps. In the application step, the aluminum is immersed in the titanate solution. The aluminum coupons, covered by a solvated titanate film, are then permitted to hydrolyze in humid air (or in various other environments), which results in the formation of a 500 to 2000 Å thick, mixed titanium-aluminum oxide. The total reaction may be written

$$2x\ AlOOH + y\ Ti(OR)_4 + (2y - x)H_2O \rightarrow xAl_2O_3 \cdot yTiO_2 + 4y\ ROH \qquad (7)$$

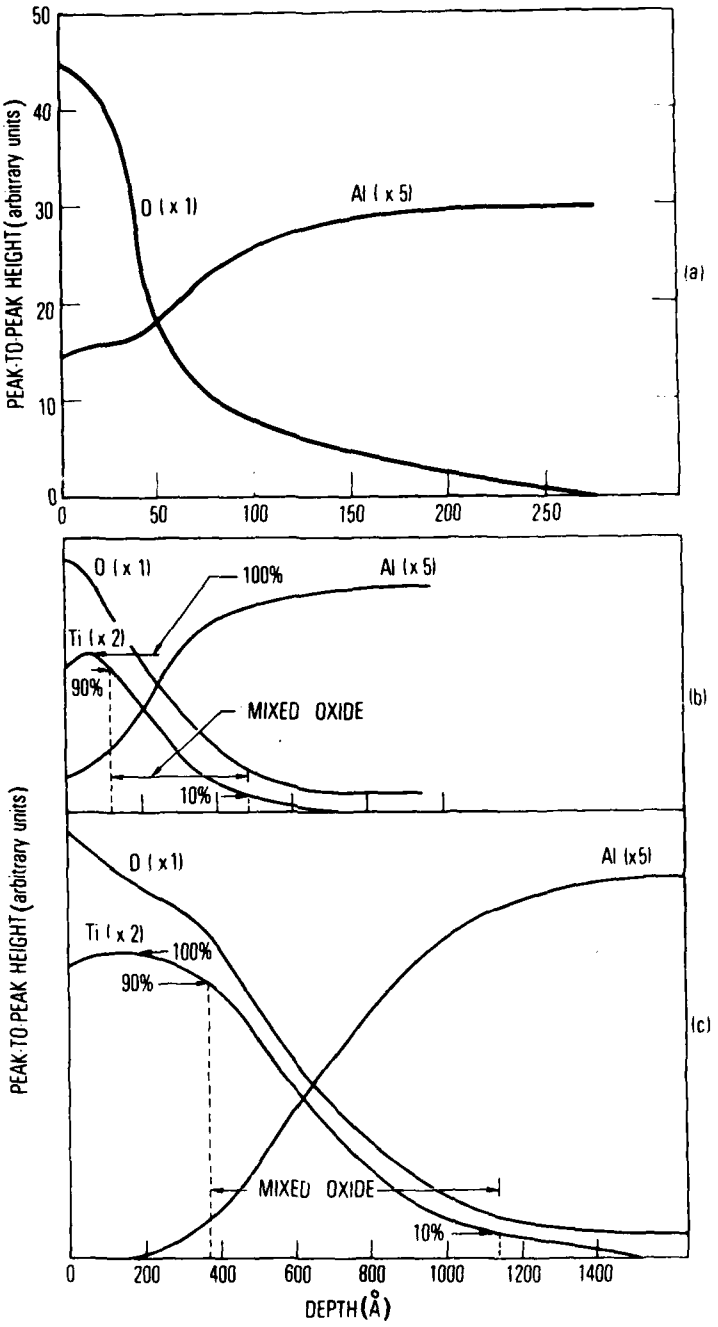

Fig. 14. Auger Depth Profiles of Titanium-Aluminum Mixed Oxide Coatings Deposited from 0.06 M TBT Solution. (a) Aluminum oxide resulting from cleaning; (b) Dry coating solution hydrolyzed in dry N_2; (c) Wet coating solution hydrolyzed in moist N_2. Note scale change for depth between (a) and (b)

where AlOOH represents the initially hydroxylated aluminum surface oxide and $xAl_2O_3 \cdot yTiO_2$ represents the mixed titanium-aluminum oxide surface. We reiterate that the titanium alkoxides have the generic formula $Ti(OR)_4$, where R is an organic group (the butyl group for the work described in this section). Properties of the coating bath (such as solvent type, residual water concentration, and the degree of polymerization of the alkoxy titanate) and properties of the hydrolysis environment (such as humidity) can affect: (a) the total film thickness; (b) the thickness of the titanium-aluminum interface region; and (c) the corrosion resistance.

The mixed titanium-aluminum oxide coatings deposited on aluminum from TBT solutions provide a thick, corrosion-resistant barrier. This surface oxide provides better corrosion protection (about 110 hr salt spray lifetime) than the thin aluminum oxide layer (less than 30 hr salt spray lifetime) that is grown in air or that forms during the cleaning procedure. The peak-to-peak intensities of the Auger electron peaks of the indicated elements are plotted against the depth into the coating in Fig. 14. The aluminum oxide grown during the cleaning procedure was only about 150 Å thick, Fig. 14(a).

The typical solution-deposited mixed titanium-aluminum oxide film consists of two regions: an interfacial region composed of a mixed oxide and an outer region that consists mainly of titanium and oxygen. The depth profiles of two typical mixed oxide coatings are shown in Figs. 14(b) and 14(c). The solution-formed coatings have broad interfacial regions consisting of mixed titanium and aluminum oxides. This mixed region is typically 60 to 90% of the entire coating. All of the solution-deposited coatings in this study had a broad interfacial region and a relatively small outer layer of titanium oxide.

1. ALUMINUM OXIDATION

Coatings hydrolyzed under conditions of 60 to 100% relative humidity, Fig. 14(c), have thicker titanium oxide and mixed oxide layers (700 Å) than coatings hydrolyzed at less than 20% relative humidity (400 Å), Fig. 14(b). Aluminum oxidation is responsible for the increase in the thickness of the mixed oxide layer. Several aluminum oxidation reactions are likely. Aluminum can react with the isopropanol solvent at room temperature to form aluminum isopropoxide (Ref. 31):

$$Al + 3\ iPrOH \rightarrow Al(OPr\text{-}i)_3 + \frac{3}{2} H_2 \qquad (8)$$

Oxygen can also form the oxide directly through cracks in the coating:

$$2\ Al + \frac{3}{2} O_2 \rightarrow Al_2O_3 \qquad (9)$$

These two reactions contribute an appreciable number of aluminum ions to the oxide since the mixed region formed under low humidity, Fig. 14(b), where these are the only oxidation mechanisms, is thicker than the original aluminum oxide, Fig. 14(a).

Water can also react with aluminum to form the hydrated oxide (Ref. 32):

$$Al + 2\ H_2O \rightarrow AlOOH + \frac{3}{2} H_2 \qquad (10)$$

This reaction can form a porous, hydrated aluminum oxide layer from a dense, barrier-type aluminum oxide (Ref. 33). The increase in porosity of the aluminum oxide may expose aluminum metal to further oxidation by water, Eq. (10), or by the solvent, Eq. (8). This porosity induced by moisture may account for the thick mixed oxide layer of coatings hydrolyzed in high humidity atmospheres, Fig. 14(c). The profile of a radio frequency (rf) sputtered titanium dioxide coating is presented in Fig. 15. This coating has a fairly sharp, mixed, oxide interface that constitutes only 30% of the total coating depth. The outer layer consists of titanium dioxide. The mixed region in the rf-deposited titanium-dioxide coatings corresponds to the original aluminum oxide produced during the surface preparation. No apparent further oxidation of aluminum occurs.

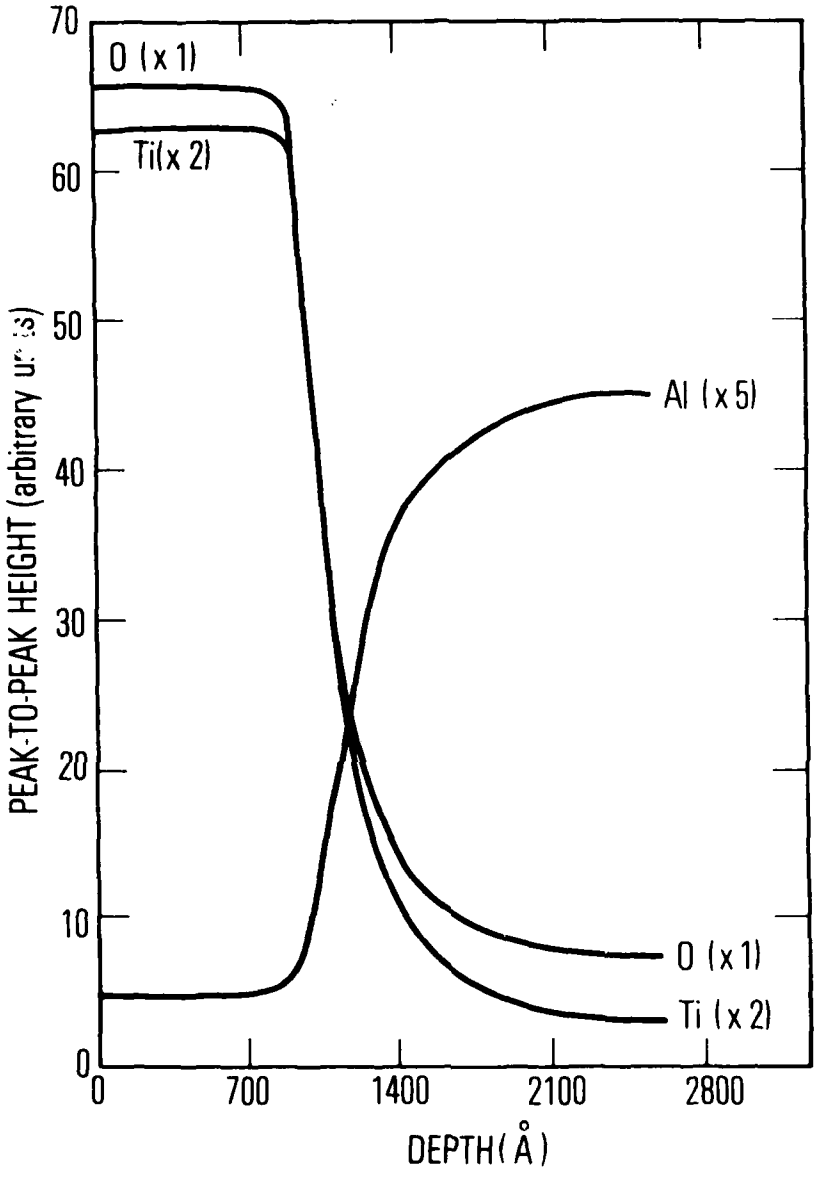

Fig. 15. Auger Depth Profile for RF-Deposited Titanium-Aluminum Oxide

Determination of the structure of the mixed titanium-aluminum oxide region depends upon the accuracy of the Auger concentration profiles. The surface roughness of the aluminum sample can broaden the apparent interfacial region. To address this issue, aluminum test coupons were chemically polished by immersion in a solution of 80.5 vol% phosphoric acid, 3.5% nitric acid, and 16% water for 20 min at 90°C (Ref. 10). These surfaces appeared smooth when observed with a scanning electron microscope at 20,000X magnification. After being polished, coupons were cleaned and coated with titanate from solution or, in some cases, were coated with titanium dioxide by rf sputtering. These coupons showed no change of surface roughness in the SEM after solution or rf deposition of titanium oxide. We conclude that surface roughness is not responsible for the broad interfaces observed in Auger concentration profiles. Since intensity profiles consistent with those obtained on unpolished specimens were obtained, specimen polishing is justifiably omitted from the usual specimen preparation procedure. The polished and unpolished coatings have similar profiles since distances characteristic of surface topographic variations on unpolished specimens are large compared with coating thicknesses. This viewpoint is supported by recently published work on the influence of surface roughness on depth profiles of gold films deposited on nickel surfaces (Ref. 34).

2. DEPOSITION AND HYDROLYSIS OF TITANATES

The thickness of the mixed oxide depends upon the coating bath and hydrolysis atmosphere conditions during the formation of the coating. The total reaction in Eq. (7) illustrates the importance of water in the formation of the mixed oxide. The effects of water in the coating solution and of water vapor in the hydrolysis atmosphere are illustrated by the data in Table 4.

The titanate starting material was used in two forms: trimeric (Ref. 28) or polymeric TBT. Trimeric and polymeric TBT applied from dry coating solutions and hydrolyzed at 100% relative humidity resulted in thick coatings (800 to 1500 Å). Coatings applied from trimeric TBT in wet coating baths (0.06 to 0.6 M H_2O) and hydrolyzed at high humidity resulted in coatings 800 to 1200 Å thick. Coatings hydrolyzed at low humidity (less than 10% relative

humidity) are thinner (500 to 700 Å) when trimeric TBT is used regardless of the concentration of water in the bath. Polymeric TBT hydrolyzed at low relative humidity (10%) forms fairly thin (600 to 900 Å) mixed oxides. The thicknesses of coatings made from polymeric TBT increase slightly with increasing concentration of water in the coating bath.

Table 4. Effect of Water and Initial Polymerization of TBT Coating Bath (0.06 M TBT in Isopropanol)

TBT Type	Relative Humidity in Hydrolysis Atmosphere (%)	Corrosion Lifetime (hr)	Thickness (Å)
	Dry Coating Bath		
Trimer	<10	50 - 60	500 - 700
	100	80 - 100	800 - 1000
Polymer	<10	80	600 - 900
	100	90 - 130	1000 - 1500
	0.06 - 0.6 M Water in Coating Bath		
Trimer	<10	60 - 70	600 - 700
	100	50 - 60	800 - 1200
Polymer	<10	80	700
	100	100	1600 - 1700

Two titanate species are formed at the aluminum-solution interface during the application step: bound and unbound TBT. TBT that reacts with the hydrated aluminum is strongly bound to the interface. TBT is probably bound to the aluminum by a reaction with hydrated aluminum oxide:

$$AlO(OH) + Ti(OBu)_4 \rightarrow O\text{-}Al\text{-}O\text{-}Ti(OBu)_3 + BuOH \qquad (11)$$

Unbound TBT can further polymerize with TBT in a series of steps. Water from the solution can partially hydrolyze the bound TBT, which results in an active hydroxide site for further addition of TBT (Refs. 22-24):

$$-OTi(OBu)_3 + H_2O \rightarrow -OTi(OBu)_2OH + BuOH \quad (12)$$

The dangling bond represents a bond to the aluminum surface or to bound surface coating. TBT from the solution can then be added to this active hydroxide site to form the next layer (Ref. 30).

$$-OTi(OBu)_2OH + Ti(OBu)_4 \rightarrow -OTi(OBu)_2OTi(OBu)_3 + BuOH \quad (13)$$

The reactions of Eqs. (12) and (13) may be repeated to buildup the bound coating. The reactions shown in Eqs. (11) through (13) for monomeric TBT can also be extended to trimeric or polymeric TBT (Refs. 23, 25-27).

The bulk of the coating that results from the application step is not tightly bound to the surface. This weakly bound, solvated layer of titanate is adsorbed over the bound titanium-aluminum alkoxide layer just discussed. The solution drains off the surface, which disturbs this solvated layer, immediately after removal of the sample from the coating bath, resulting in thin coatings. This unconsolidated outer layer can be removed by briefly dipping the specimen in an isopropanol bath immediately after removal from the coating bath. Very thin coatings (200 Å) containing some titanium resulted after hydrolysis of these washed coatings prepared from 0.06 M TBT in isopropanol, whereas coatings formed by the same procedure but not rinsed are typically thicker (greater than 400 Å).

High humidity can quickly polymerize the unconsolidated layer to yield thick, mixed oxides. Adsorbed trimeric TBT is polymerized at high humidity, and thick coatings result (Table 4). These observations illustrate that most of the titanium that eventually becomes part of the hydrolyzed coating is initially only weakly associated with the surface. Most of the important hydrolysis reactions that determine the ultimate thickness and corrosion resistance of the oxide film involve this initially unconsolidated or gelatinous layer. Much of this associated layer drains off during hydrolysis at low humidity of coatings formed from trimeric TBT, and thin films result. Polymeric starting material is more strongly adsorbed so that these coatings are less affected by runoff at low humidity than the trimeric material (Table 4).

The solvent used in the coating bath can control the water required to hydrolyze the TBT in the liquid surface film. Table 5 indicates that only thin (600 to 700 Å) coatings are formed from trimeric TBT in dry toluene in both high- and low-humidity atmospheres. Corrosion resistance increases moderately with increased humidity for toluene solvent, whereas both the corrosion resistance and the thickness increase with humidity when isopropanol is used as the solvent (Section V.I). The thickness of the coating probably is controlled by the amount of TBT that becomes bound at the interface. The low solubility of water in toluene and the relatively slow rate of evaporation of toluene permit the loss of unconsolidated TBT by solution runoff since the TBT is polymerized slowly. Isopropanol evaporates more quickly and is a better solvent for water. Thus, water diffuses rapidly into the solution, polymerizes the TBT, and binds the polymer, which results in a thick coating. The corrosion resistance of coatings applied with the use of both isopropanol and toluene solvents is enhanced by hydrolysis in very humid atmospheres since water can seal reactive faults in the oxide and ensure that the alkoxide is fully hydrolyzed.

Table 5. Solvent Effects on TBT Coatings (Coating Bath 0.06 M TBT)

Solvent	Relative Humidity in Hydrolysis Atmosphere (%)	Salt-Spray Lifetime (hr)	Coating Thickness (Å)
Dry isopropanol	<10	50 - 60	500 - 700
Dry isopropanol	100	70 - 100	700 - 1000
Dry toluene	10	40 - 50	600 - 700
Dry toluene	100	70	600 - 700

Coating thickness is weakly dependent upon the oxygen concentration in the coating solution and in the hydrolysis atmosphere (Table 6). The role of oxygen was investigated by forming coatings in nitrogen- or air-saturated

0.06 M solutions of TBT in isopropanol. Coatings hydrolyzed in air are thicker but slightly less corrosion resistant than coatings hydrolyzed in nitrogen (Table 6). Oxygen plays only a minor role in coating formation in wet atmospheres. Data in Table 6 for hydrolysis in dry atmospheres indicate that oxygen can increase the thickness of the interface, Eq. (9). Oxygen does not react with the alkoxide to further seal or crosslink the oxide, and the corrosion resistance does not increase.

Table 6. Effect of Oxygen on TBT Coatings During Application Step and Hydrolysis

Hydrolysis Conditions	Ambient Atmosphere Over Coating Bath	Corrosion Lifetime (hr)	Coating Thickness (Å)
Stagnant N_2	N_2	90	1000
Stagnant N_2	Air	80	1100
Stagnant air	N_2	80	1100
Stagnant air	Air	70	1300
Flowing N_2	Air	40	400
Flowing air	Air	30	700

[a]Coatings were deposited by coating test coupons in 0.06 M TBT in wet isopropanol saturated with the indicated gas and hydrolyzing in trapped or flowing (but nonrecirculated) gas as indicated.

The immersion time and temperature of the bath do not affect final properties of mixed oxide coatings. Samples coated for 10 sec to 30 min did not show any differences after hydrolysis. Coatings formed from 0.06 M TBT solutions in isopropanol at 82°C were similar to coatings formed at room temperature.

These data support our concept that during the coating application step, a primarily unconsolidated film of TBT and solvent are deposited on the aluminum surface, and only a small portion of the coating is bonded to the

interface. The dissolved oxygen concentration in the solvents was not a major factor in the formation of the coating. The hydrolysis of the coating is mainly controlled by the concentration of water in the hydrolysis atmosphere; thick, corrosion-resistant coatings are obtained at high relative humidity. At low relative humidity, oxidation of aluminum by oxygen can form thicker coatings than coatings formed in dry nitrogen atmosphere; however, poor corrosion resistance results in both cases since sufficient water is required in the hydrolysis atmosphere for the sealing of the coating.

Corrosion resistance and oxide thickness are primarily determined by the availability of water in the coating and hydrolysis steps. Apparently water causes oxidation of aluminum, which increases the thickness of the mixed oxide interfacial region of the coating. TBT is presumed to bond to this hydrated layer of aluminum oxide. Additional solvated TBT is adsorbed on this layer, and rapid hydrolysis is required to avoid loss of this loosely bound solvated layer. Water in the hydrolysis atmosphere probably diffuses into the solvated layer and polymerizes the organic titanate, binding it more strongly to the surface. Use of prepolymerized TBT results in a more strongly bound solvated layer. Thus, only a small amount of titanate is lost due to runoff even in dry atmospheres, and thicker coatings result. The prepolymerized solvated layer becomes bound to the surface during hydrolysis, and the product alcohol evaporates as the solvent evaporates. A stable titanium-aluminum mixed oxide results, which contains an outer layer of titanium dioxide from the polymerized TBT and an inner layer of titanium-aluminum mixed oxide. Cracks in the coating are sealed by water, which forms oxo-bridges between titanium atoms that provide good corrosion resistance.

VI. FORMATION AND CHARACTERIZATION OF OTHER OXIDE SYSTEMS

Although most of our work has been concerned with the chromate and titanate systems, several other mixed oxides were also studied. It is convenient to classify coating systems as being either of the type in which the valence of the deposited species changes or of the type in which there is no change in cation valence. The chromate system constitutes an example of the first type; Cr^{+6} ion is reduced to Cr^{+3}. In contrast, in the titanate system, titanium formally remains in the +4 valence state. We shall now examine further examples of each type of coating.

A. COATING SYSTEMS WITHOUT CHANGE IN CATION VALENCE

1. SILICON DIOXIDE COATINGS

Silicon dioxide is an inert, stable substance, and its use in corrosion-protective films suggests itself. Silicon compounds, in the form of silicone resins, are used as protective coatings in various applications. Recently, a new silicone coating formulation (VESTAR^{TM}), offering superior corrosion protection to light metals, has become commercially available (Ref. 35). This coating consists of colloidal silica and a partially condensed silanol in an acidified water and alcohol solvent. The silica provides a high degree of abrasion resistance. Our approach to the formation of SiO_2 coatings is quite different. It follows to some extent the approach taken with the TiO_2 coatings previously described.

a. Coatings Formed from $SiCl_4$

Silicon tetrachloride is easily hydrolyzed to form a silicon oxide coating. Solutions of 0.5 to 1.0 vol% of $SiCl_4$ in toluene were studied. Coatings hydrolyzed slowly in closed containers showed small pits due to attack by HCl. Rapidly hydrolyzed coatings showed no initial pitting and had a salt spray lifetime of 100 to 170 hr. More concentrated solutions of 15 to 100 vol% $SiCl_4$ in toluene showed some pitting when rapidly hydrolyzed and were less durable (40 to 70 hr of salt spray lifetime). All coatings exhibited an outer SiO_2 layer constituting 30 to 50% of the total coating thickness. The

remaining part of the coating consisted of a mixture of silicon and aluminum oxides with increasing aluminum concentration toward the substrate. A typical depth profile of an SiO_2 coating formed from $SiCl_4$ is shown in Fig. 16(a). Experimental results are summarized in Table 7. The coatings appear to be fully hydrolyzed since no peak for chlorine is observed, as is evident in the complete Auger spectrum of Fig. 16(b).

The experimental data suggest that the $SiCl_4$ reacts with the hydrated surface of the aluminum oxide according to the reaction

$$AlOOH + SiCl_4 \rightarrow -AlOOSiCl_3 + HCl \qquad (14)$$

Additional layers are added to the coating by a two-step reaction sequence involving water

$$-O-SiCl_3 + H_2O \rightarrow -OSiCl_2OH + HCl \qquad (15)$$

$$-O-SiCl_2OH + SiCl_4 \rightarrow -OSiCl_2OSiCl_3 + HCl \qquad (16)$$

where the "dangling" bond symbol again implies a bond with the substrate. The use of a solvent that does not react with $SiCl_4$ (e.g., toluene) is assumed. After removal from the coating bath, it is believed that the coated aluminum hydrolyzes according to the reaction as the solvent evaporates and water diffuses into the coating.

$$-OSiCl_2O- + H_2O \rightarrow -"SiO_2-" + 2HCl \qquad (17)$$

b. Coatings Formed from Silicon Tetraethoxide

Silicon ethoxide, $Si(OEt)_4$, is not hydrolyzed by water; a stronger base is required. Aluminum test coupons (AA 1100) were coated using 2% solutions of $Si(OEt)_4$ in either methanol or toluene with varying amounts of either NaOH or KOH, and water. Data obtained for silicon oxide coatings deposited from various solvents with different hydroxide concentration are summarized in

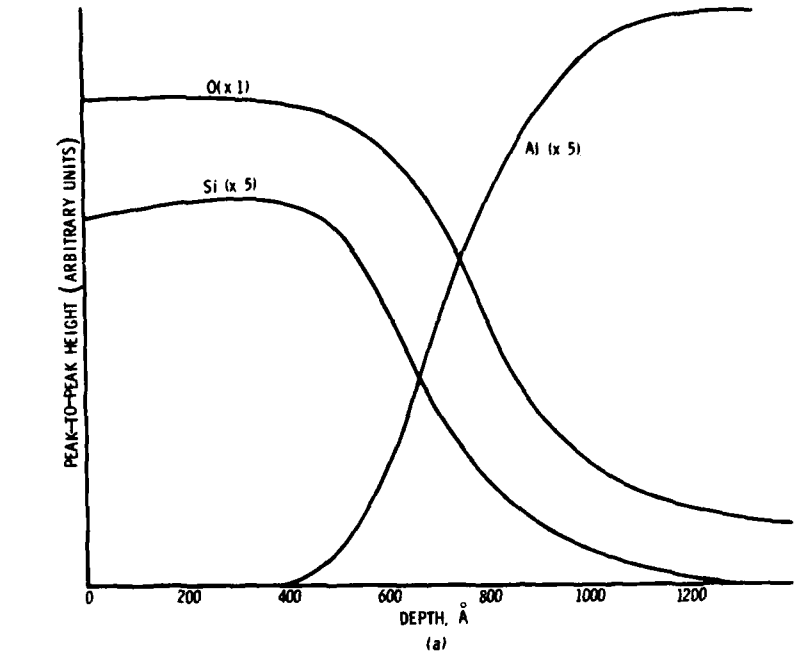

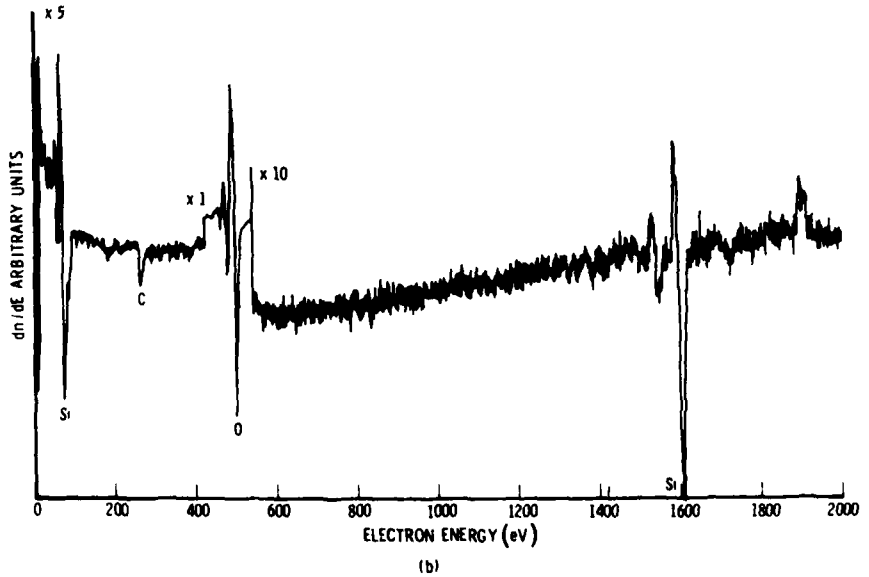

Fig. 16. Silicon-Aluminum Mixed Oxide Coatings Formed from $SiCl_4$. (a) Typical Auger depth profile; (b) Complete Auger spectrum

Table 7. Characteristics of Coatings Formed from $SiCl_4$

Auger Measurements		
Vol% $SiCl_4$	Coating Thickness (Å)	Mixed Oxide (%)
0.5	500	70
1 - 50	1000 - 1100	45 - 55
100	1500	60

Salt Spray Measurements	
Vol% $SiCl_4$	Salt Spray Lifetime (hr)
0.5 - 1	100 - 170
25 - 100	40 - 70

Table 8. The concentration of sodium or potassium in the coating increases with increasing water or base concentration in the solvent. Water seems to produce a thicker (but perhaps less dense) coating with intermediate corrosion protection (approximately 60 hr salt spray exposure).

It is proposed that the first layer of $Si(OEt)_4$ bonds to the hydrated surface aluminum oxide

$$AlOOH + Si(OEt)_4 \rightarrow AlOO\text{-}Si(OEt)_3 + EtOH \quad (18)$$

We believe that the hydroxide ion catalyzes the polymerization of $Si(OEt)_4$ both on the surface and in solution faster than it (the OH^-) attacks the surface according to the sequence of reactions

$$-OSi(OEt)_3 + OH^- \rightarrow -OSi(OEt)_2OH + EtO^- \quad (19)$$

$$-OSi(OEt)_2OH + Si(OEt)_4 \rightarrow -OSi(OEt)_2OSi(OEt)_3 \quad (20)$$

$$EtO^- + H_2O \rightarrow EtOH + OH^- \quad (21)$$

Table 8. Characteristics of Coatings Formed from $Si(OEt)_4$ (2%)

Solvent	Base Conc. (wt%)	Base	H_2O (%)	Salt Spray Lifetime (hr)	Coating Thickness (Å)	Percent Mixed Oxide (%)	Absolute Auger Amplitude- Na or K Signal
Methanol	0.001	-	1.0	20	150 - 170	Al_2O_3 only	-
Methanol	0.005	NaOH	0.0				0.5
Methanol	0.05	NaOH	0.0			80	0.7
Toluene	0.2	KOH	0.3	70	360 - 380		4.5
Methanol	0.5	NaOH	0.0	80		60	1.4
Methanol	0.5	NaOH	10.0	60	1800	70	4.3
Toluene	0.9	KOH	1.0		2050	40	6.6

Hydrolysis of the gelatinous, partially organic layer then results in a compact coating with the outer 40% of its total thickness in the form of "SiO_2" and the remainder a mixed aluminum-silicon oxide. Partially polymerized $Si(OEt)_4$ in the coating solution may also deposit on the surface and results in a better coating since some organic groups will already have been removed.

c. Coatings Formed from Mixtures of $SiCl_4$ and $Si(OEt)_4$

Mixtures of $SiCl_4$ and $Si(OEt)_4$ are somewhat less corrosive to aluminum than is $SiCl_4$ alone, although some pitting occurs for slow hydrolysis after coating by solutions with more than 0.05 vol% of $SiCl_4$. Rapid hydrolysis produces fairly durable (approximately 100 hr salt spray lifetime) and thick (about 1500 Å) coatings with only a small mixed oxide region (approximately 44% of the total coating thickness) for a mixture of 1 vol% $SiCl_4$ and 1 vol% $Si(OEt)_4$ in toluene (see Table 9). The depth profile for a coating formed from an $SiCl_4/Si(OEt)_4$ mixture, shown in Fig. 17, is very similar to the $SiCl_4$ profile shown in Fig. 16a.

Table 9. Characteristics of Coatings Formed from $SiCl_4/Si(OEt)_4$ Mixtures

Vol% $SiCl_4$	Vol% $Si(OEt)_4$	Salt Spray Lifetime (hr)	Coating Thickness (Å)	Mixed Oxide (%)
0.05	0.05	30	400	60
0.05	0.5	50	780	50
0.5	0.05	50	670	50
0.5	0.5	60	500	60
1.0	1.0	30	600	60
1.0	1.0	100	1500	40
2.0	2.0	40	1150	90
4.0	4.0	60	670	60

All coating mixtures in toluene solvent.

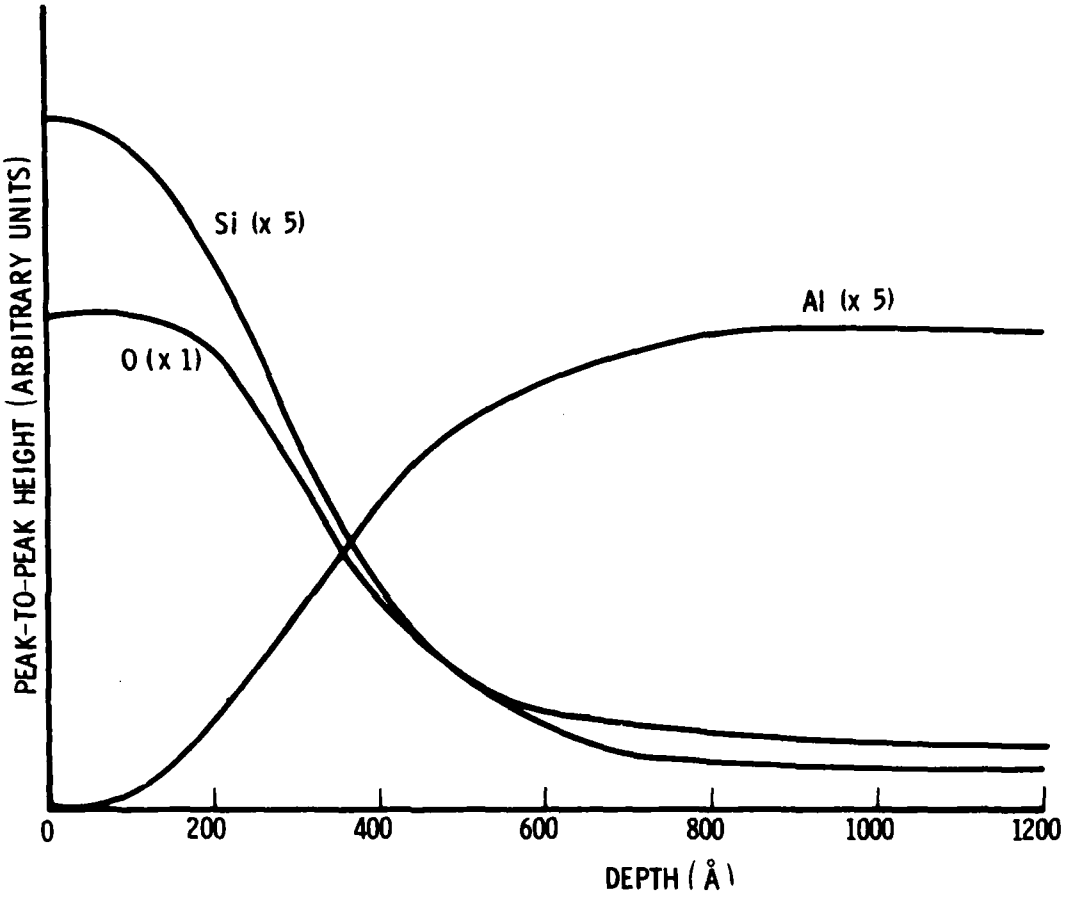

Fig. 17. Auger Depth Profile of Silicon-Aluminum Mixed Oxide Formed from $SiCl_4/Si(OEt)_4$ Mixture

3. ZIRCONIUM DIOXIDE COATINGS

Zirconium dioxide was successfully deposited from toluene solutions of zirconium tetra isopropoxide (10 g/liter) and zirconium tetra n-propoxide (2% by volume). The coated aluminum coupons were hydrolyzed in air. Auger analysis showed that this coating procedure results in a region of mixed zirconium/aluminum oxide about 1000 Å thick; however, this film is apparently not insoluble in water, and corrosion resistance is minimal. Since the anhydrous aluminum oxides are inert and insoluble, this observation can only be explained by the incorporation of water into the film. However, heating the test coupons to approximately 500°C did not improve their corrosion resistance.

4. INDIUM OXIDE COATINGS

Indium oxide films were deposited from solutions of indium pentane dionate (10 g/liter) in toluene. The films were thin, with poor corrosion resistance (about 30 hr salt spray lifetime).

5. TANTALUM OXIDE COATINGS

Fairly thick (1200 Å) films of tantalum oxide were deposited from a 2 vol% solution of $Ta(OC_2H_5)_5$ in isopropanol. About 90% of the thickness of these films is a region of mixed tantalum and aluminum oxides. Preliminary tests indicate a salt spray lifetime of only about 30 hr, but the system may merit further study on the basis of the performance anticipated from the conceptual model.

B. SYSTEMS WITH CHANGE IN CATION VALENCE

Film-forming cations in this category can actively oxidize aluminum metal, and thus can potentially create a thick region of mixed oxide. As previously mentioned, the chromate conversion coatings are prime examples of this type of system. Chromate coatings are of course widely employed; they are currently used to treat Air Force aircraft. Several of the elements near chromium in the periodic chart also occur in compounds with high formal valence states and considerable oxidizing power, and have stable lower valence states. Such elements have the potential of forming useful corrosion

protective oxide barriers on aluminum. We have studied vanadium coatings fairly extensively and have examined manganese, molybdenum, and niobium to a lesser degree. Although these materials do not necessarily require organic solvents for application, the experiments have been primarily with metal alkoxides in organic solvents.

1. VANADIUM OXIDE COATINGS

Coating solutions were either $VO(OC_3H_7)_3$ or $VO(OC_4H_9)_3$ (both formally pentavalent compounds) in toluene, isopropanol, or butanol solvent. Typically, aluminum coupons were immersed in the dilute alkoxide solution, then withdrawn to permit the residual alkoxide to hydrolyze.

The rate of hydrolysis of the iso-propoxide is much more rapid than that of the n-butoxide because of the smaller relative sizes of the alkoxide groups. A comparison of coupons allowed to stand in air and in dry N_2 showed a mixed oxide layer approximately 500 Å thick in both cases; however, the total amount of vanadium was much greater on those coupons hydrolyzed quickly in air, see Figs. 18(a) and 18(b). Corrosion resistance was also slightly greater for these coupons than for coupons hydrolyzed in nitrogen, although only half as great as for chromate coatings. Excess vanadium oxide on the surface seems to offer little additional corrosion protection since it is slightly water soluble.

Analysis of vandium coatings by XPS indicates that vanadium is either pentavalent or trivalent, but not quadrivalent (Ref. 36). The colors of the vanadium oxides are: V_2O_5, yellowish red; VO_2, blue; V_2O_3, black; and VO, light grey. The deposited coatings are rather green in color. Coupons heated in air to 500°C turned yellow. We have tentatively classified the vanadium system as one in which the cation changes valence state. Our results could, however, be explained by the presence of a pentavalent hydrated form.

The most successful vanadium coatings were produced by initially boiling aluminum coupons in distilled water. Auger analysis shows that boiling the aluminum produces a thick (2000 to 3000 Å) film of (hydrated) aluminum oxide. After treatment with a dilute solution of vanadium alkoxide, Auger analysis shows penetration of vanadium to a depth of approximately 200 Å into the

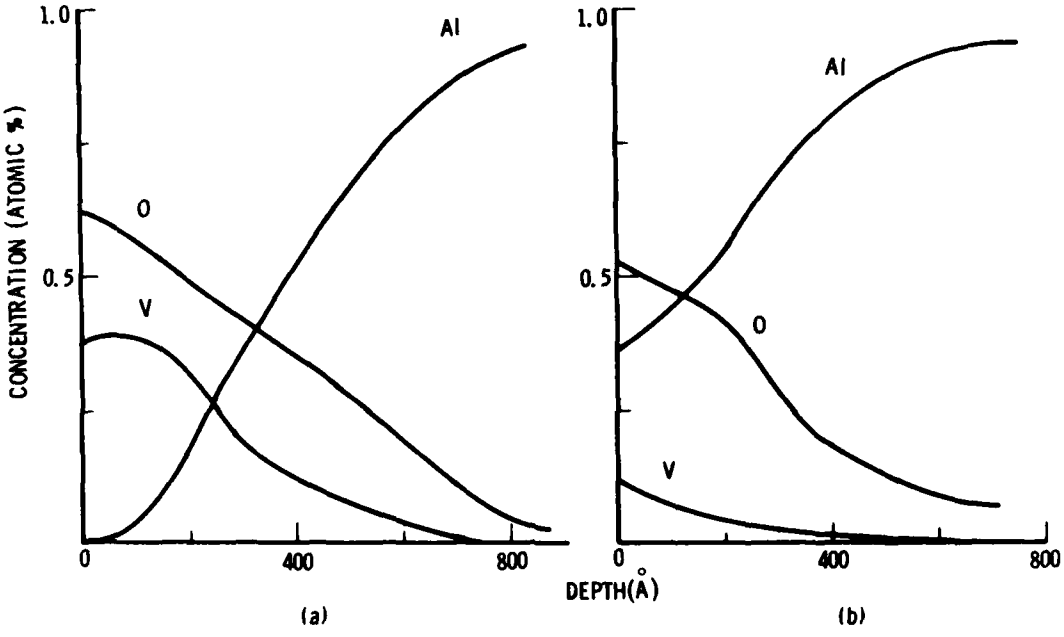

Fig. 18. Auger Depth Profiles for Vanadium-Aluminum Mixed Oxide Coatings. (a) Hydrolyzed in air; (b) Hydrolyzed in dry N_2

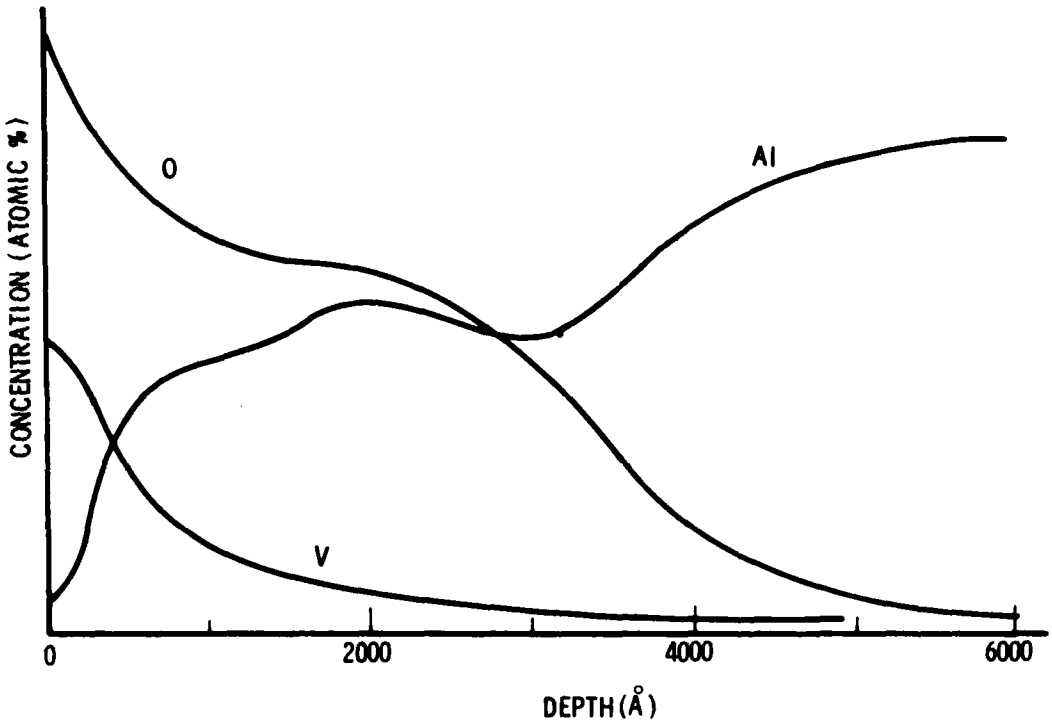

Fig. 19. Auger Depth Profile of Vanadium-Aluminum Mixed Oxide Coating Grown on Aluminum Boiled in Distilled Water

aluminum oxide film (Fig. 19). Coatings so prepared have a salt spray lifetime about two-thirds that of chromate coatings (i.e., 100 hr), but approximately twice that of coupons that have only been boiled.

2. MANGANESE OXIDE COATINGS

Manganese oxide coatings were formed by suspending aluminum coupons in dilute (5 g/liter) solutions of $KMnO_4$ for about 24 hr. After immersion, the aluminum test coupons appeared to be light golden brown in color. Auger analysis indicated an aluminum-manganese mixed oxide film about 500 Å thick (Fig. 20). Salt spray corrosion lifetimes were on the order of 50 hr.

3. MOLYBDENUM OXIDE FILMS

We have produced 500 Å films of mixed aluminum-molybdenum oxides, starting with molybdenum oxychloride ($MoOCl_4$) or bis(2,4 pentanedionato) bis-oxo-molybdate (VI) ($MoO_2(C_5H_7O_2)_2$). The molybdenum oxychloride was reacted with excess isopropanol, and the HCl that evolved was neutralized with NH_3. The surface oxide produced on the test coupons was only a few hundred angstroms thick and exhibited minimal corrosion resistance. Coatings were also formed from solutions of $MoO_2(C_5H_7O_2)_2$ in toluene (10 g/liter). An Auger depth profile is shown in Fig. 21.

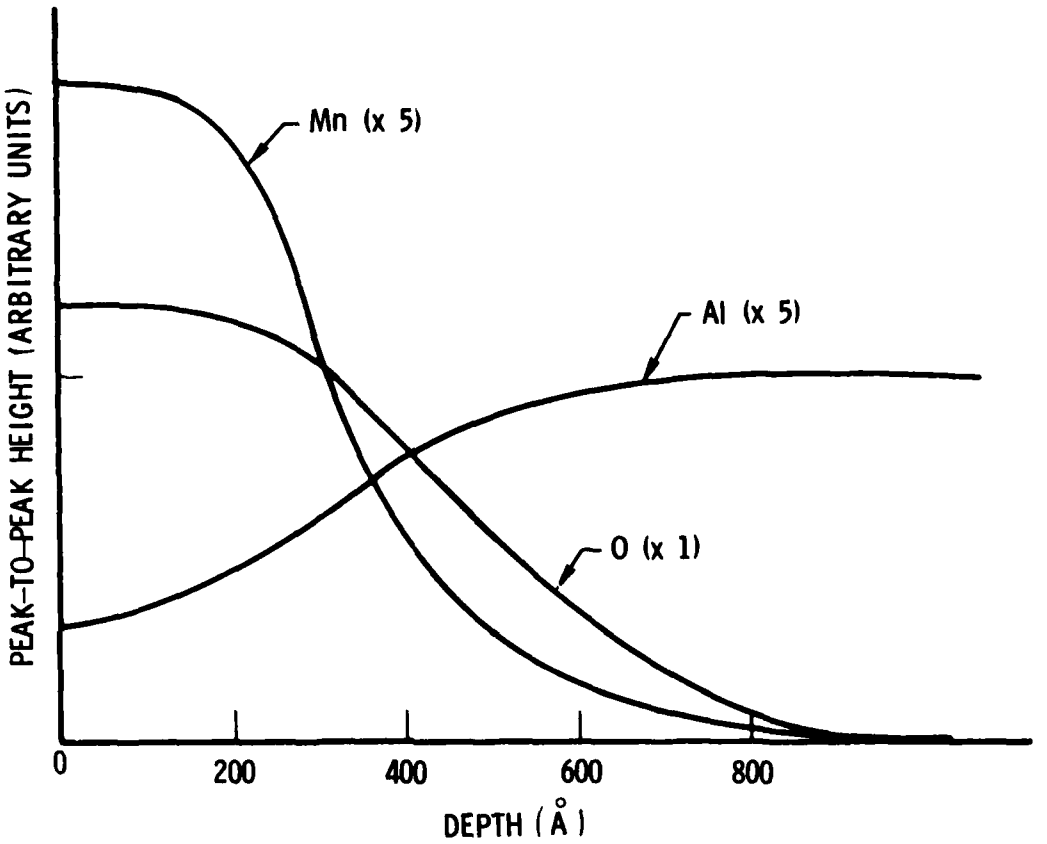

Fig. 20. Auger Depth Profile of a Manganese-Aluminum Mixed Oxide Coating

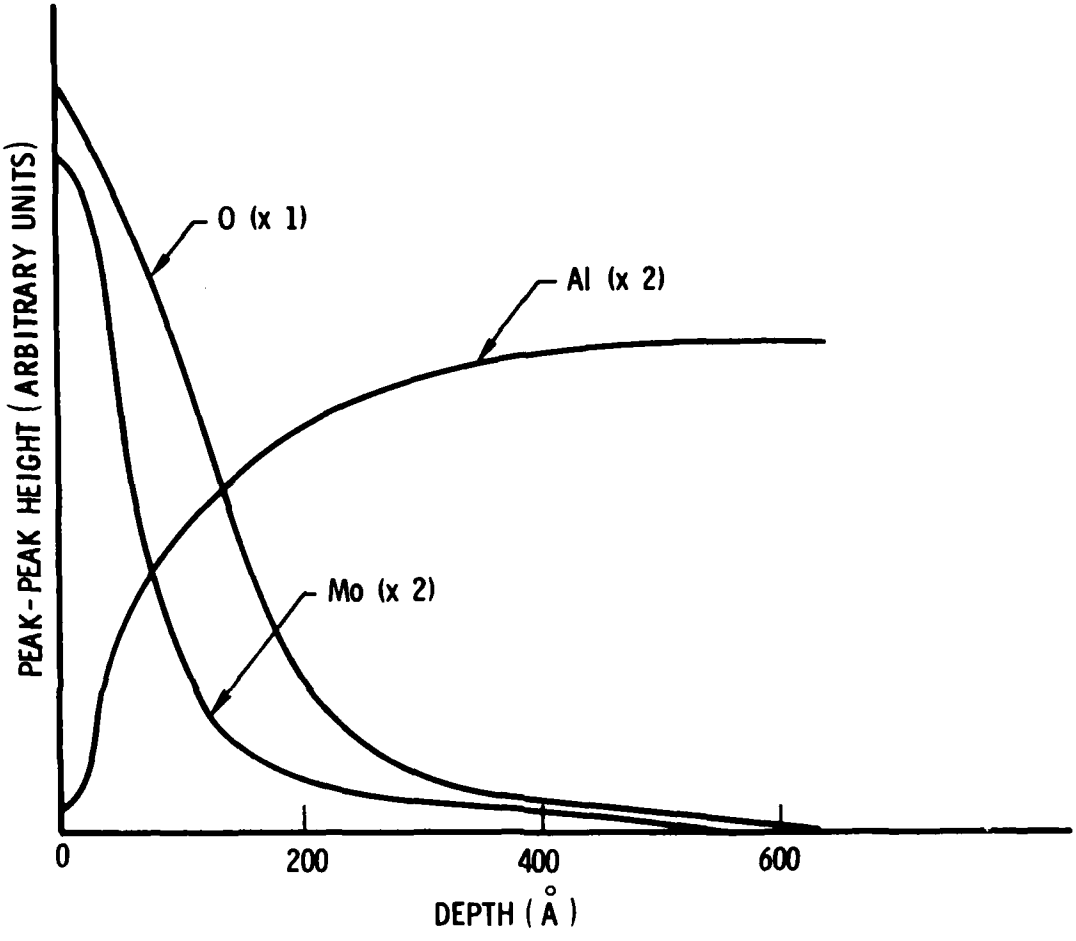

Fig. 21. Auger Depth Profile of a Molybdenum-Aluminum Mixed Oxide Coating

VII. CORROSION PROTECTION BY DEPOSITED OXIDE COATINGS

It is convenient to consider together the corrosion mechanisms operating with the different mixed oxides studied. The performance of the chromate coatings provides a useful baseline for the evaluation of the other coating types.

As stated, most of our work leading to the elucidation of coating mechanisms was performed using commercially pure or high purity aluminum. The general mechanisms of film formation are unchanged when coatings are deposited on aluminum alloy substrates. Corrosion resistance, however, is greatly affected by minor alloy constituents.

A. COATINGS ON UNALLOYED ALUMINUM

1. CHROMATE COATINGS

Auger depth profiles for samples of the STC coating after various residence times in the salt-fog chamber are categorized into three main groups. These profile types are associated with different stages of film breakdown. After 80 (±40) hr in the salt-fog chamber, there is no visible change in appearance of the coating. The Auger depth profile (Fig. 22) shows that the coatings are uniformly thinned by approximately 200 Å. The amount of fluoride detected throughout the coating is decreased, suggesting that the fluoride helps the dissolution. After 175 (±25) hr in the salt-fog, there is still no visible change in appearance. However, the depth profile (Fig. 23) shows that some of the chromium is leached from the coating, which is replaced by aluminum from the bulk. X-ray photoelectron spectroscopy indicates that more than 90% of the remaining chromium is trivalent, so it is mostly the hexavalent chromium that is being leached away. A small amount of chlorine (<1%) is detected on the surface and to a depth of approximately 200 Å. Next (after 225 ± 25 hr), there is slight visible corrosion, and the corrosion product is aluminum oxide. No trace of chlorine or fluorine is detected in these corroded areas.

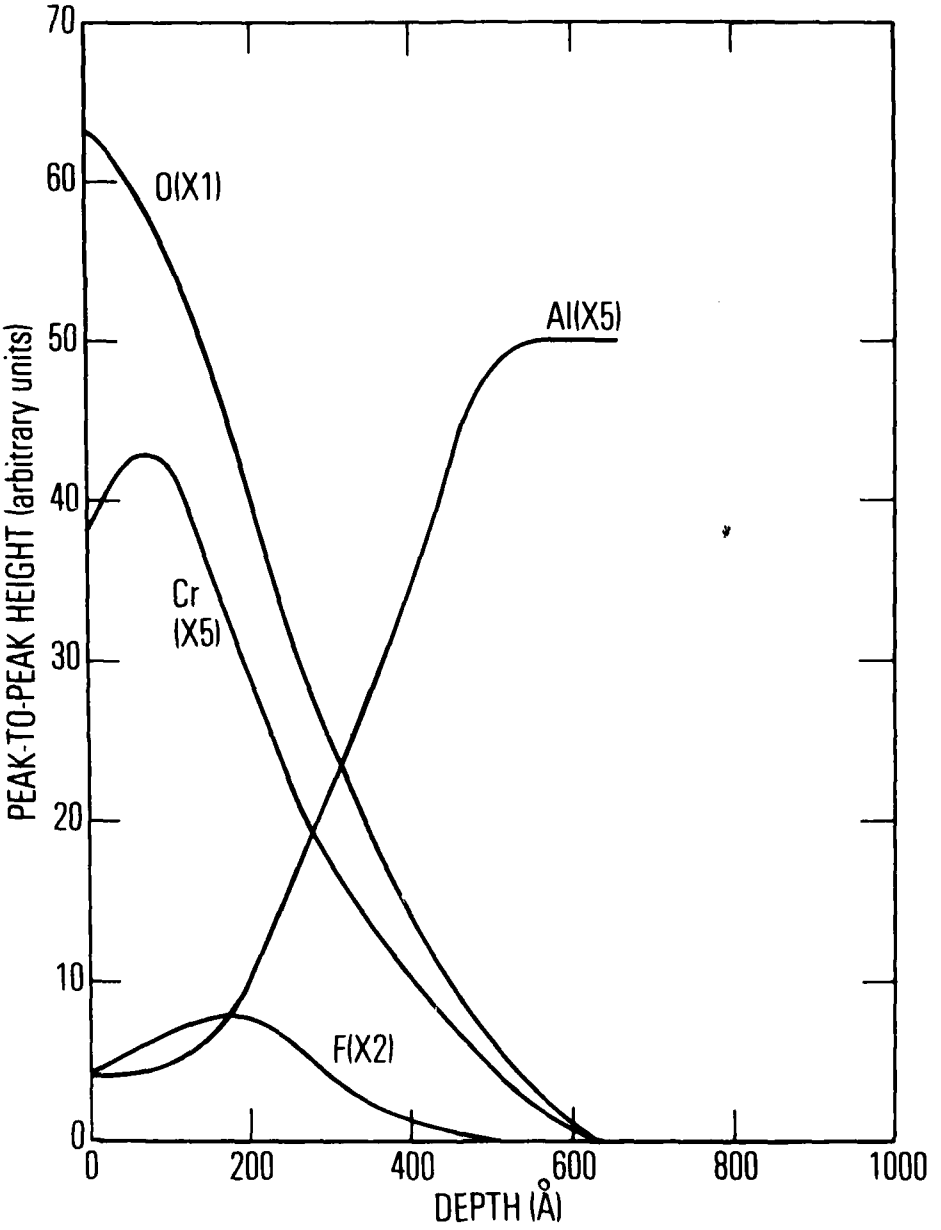

Fig. 22. STC Coating After 80 (±40) hr in Salt-Fog Chamber

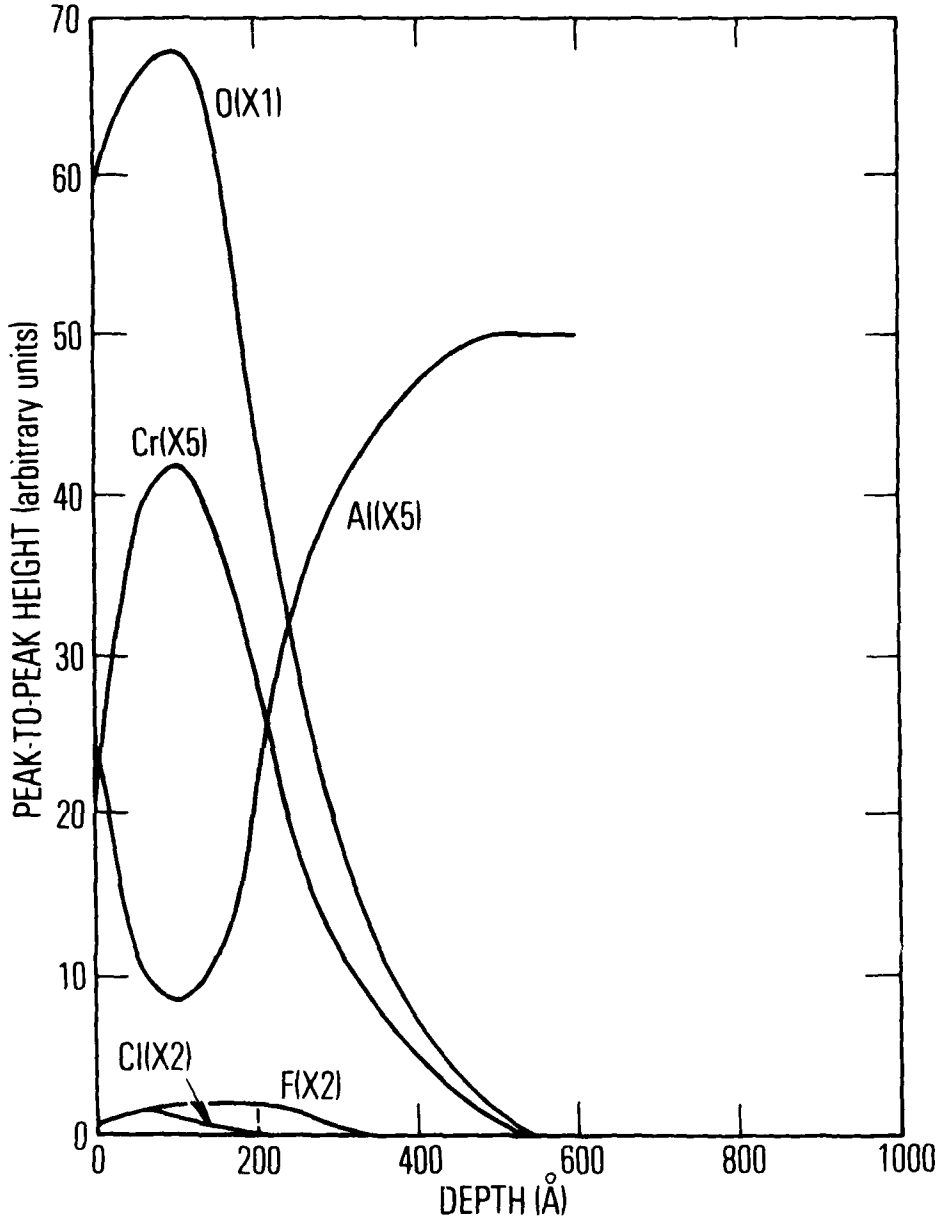

Fig. 23. STC Coating After 175 (±25) hr in Salt-Fog Chamber

All of the STC samples prepared between 25 and 40°C exhibit similar corrosion protection (visible corrosion in 200 to 250 hr). Since the thicknesses of these samples vary from approximately 450 to 750 Å, the corrosion protection probably is not strongly dependent on the coating thickness. We believe that the corrosion resistance is due mainly to the insolubility and impervious nature of the amorphous hydrated chromium oxide layer. It is less soluble than AlOOH, and, since all "weak spots" and channels are clogged with CrOOH, it is more impervious to attacking ions. The strong adhesion of the coating to the metal probably is due to the similarity in ionic radii between Al^{+3} and Cr^{+3} ($r_{Al^{+3}} = 0.50$ Å) and $r_{Cr^{+3}} = 0.53$ Å) (Ref. 37) since AlOOH coatings are known to adhere strongly to aluminum metal.

2. TITANATE COATINGS

Corrosion of titanate coatings follows a pattern quite different from corrosion of chromate coatings. Whereas chromate coatings thin fairly uniformly prior to the onset of visible corrosion, the titanium-aluminum oxide coating actually thickens during corrosion, with leaching of surface titanium and diffusion of aluminum through the oxide layer. Differences in salt spray corrosion behavior are observed between commercially pure aluminum and high-purity aluminum.

The results of a series of experiments that test titanate coatings on commercially pure (AA 1100) aluminum and on 99.999% pure aluminum with the use of the two different acid cleaning procedures are summarized in Table 10. Commercially pure aluminum (AA 1100) can contain up to 0.2 wt% copper and other impurities, which can segregate on the surface. The nominal composition of AA 1100 (with some aluminum alloys of subsequent interest) is presented in Table 11. Chromate cleaning removes both aluminum and trace copper (less than 0.2% in the bulk) and results in a surface that has no detectable copper LMM peak (917 eV) in the Auger electron spectrum. Use of the commercial aluminum cleaner Alumiprep (Aluminum Products), which contains phosphoric acid and a detergent, results in a detectable Auger copper peak due to the concentration of copper on the surface by the preferential dissolution of the aluminum.

Table 10. Effect of Acid Cleaning Step on Aluminum Corrosion

Aluminum Specimen	Surface Treatment	Corrosion Lifetime (hr)	Coating Thickness (Å)
99.999%	Uncoated	40	-
99.999%	Precleaned with chromate and coated	95	400
99.999%	Precleaned with Alumiprep and coated[a]	85	400
AA 1100	Uncoated	<20	-
AA 1100	Precleaned with chromate and coated[a]	45	700
AA 1100	Precleaned with Alumiprep and coated[a]	20	500

[a]Titanium oxide coatings deposited from 0.06 M $Ti(OBu)_4$ in isopropanol and hydrolyzed in room air.

Both the Alumiprep and the chromate cleaning procedures were efficacious for pure (99.999%) aluminum, but the chromate cleaner resulted in more corrosion-resistant coatings on commercially pure aluminum. Auger analysis of cleaned, uncoated coupons indicated that the chromate cleaning procedure removed surface copper and did not result in any residual chromium on the surface, i.e., the titanate coatings prepared in this way were not actually chromate coatings in disguise. The surface compositions of AA 1100 aluminum coupons cleaned by the two methods differed only in the amounts of surface copper. These experimental results confirmed the postulate that concentrations of segregated surface copper greater than about 5% of a monolayer result in poor corrosion resistance of titanate coatings.

Table 11. Aluminum Alloy Compositions (Typical)

Alloy Designation (AA No.)	Constituent Concentrations (wt%)								Total Max Alloy (wt%)
	Si	Fe	Cu	Mn	Mg	Zn	Cr	Ti	
1100	1.0 (Si+ Fe)		0.05 - 0.20	0.05		0.10			1.35
2024	0.50	0.50	3.8 - 4.9	0.3 - 0.9	1.2 - 1.8	0.25	0.10		8.95
6061	0.40 - 0.80	0.7	0.15 - 0.4	0.15	0.8 - 1.2	0.25	0.25	0.15	3.9
7075	0.40	0.50	1.2 - 2.0	0.30	2.1 - 2.9	5.1 - 6.1	0.18 - 0.35	0.20	12.75

Trace surface copper may aid in the growth of fairly thick coatings on AA 1100 aluminum; however, it also accelerates corrosion of these coatings. The copper segregated on the surface provides cathodic sites for the reaction of the water and titanium alkoxides. Aluminum is oxidized from the metal surface. These ionic species can migrate and either form a thick, mixed, oxide interface during coating and hydrolysis or diffuse through the coating and result in corrosion in the presence of salt-fog spray. The fate of these ions is determined by the availability of water and by the electric field produced by ions adsorbed on the coating. Wet conditions in the presence of chloride in the salt-fog spray cause aluminum ion diffusion through the coating. Corrosion of the coated surface results. Coatings grown on 99.999% pure aluminum, washed with chromate or Alumiprep, are thin, but exhibit long salt-spray lifetimes because the purity of the aluminum eliminates galvanic effects. The coatings are thin, dense, and corrosion resistant.

No problems were encountered with the adhesion of the mixed oxide films. Aluminum oxide strongly adheres to aluminum, and the mixed coating retains this property.

Figure 24(a) is a depth profile of a coating prepared from 2% TBT before exposure in the salt-fog chamber. The coating is about 1200 Å thick. After the coating remained for 20 hr in the salt-fog chamber, the profile in Fig. 24b indicates removal of some titanium from the outer surface of the coating, diffusion of some aluminum through the coating, and a thickening of the coating to about 1400 Å. After 90 hr, Fig. 24(c), an aluminum oxide layer is being formed over the original titanium mixed layer, and the coating has thickened to about 2800 Å. The coating is probably very porous at this time since there are extensive gray-colored areas on the coupon. The porous structure of this salt-fog grown aluminum oxide is probably similar to the structure reported by Hunter and Fowler for moisture-grown aluminum oxide over air-formed aluminum oxide films (Ref. 33).

The corrosion mechanism of thick (greater than 600 Å), mixed titanium-aluminum oxide coatings on aluminum substrates proceeds in three steps. Titanium is first removed from the outer part of the coating. Aluminum is

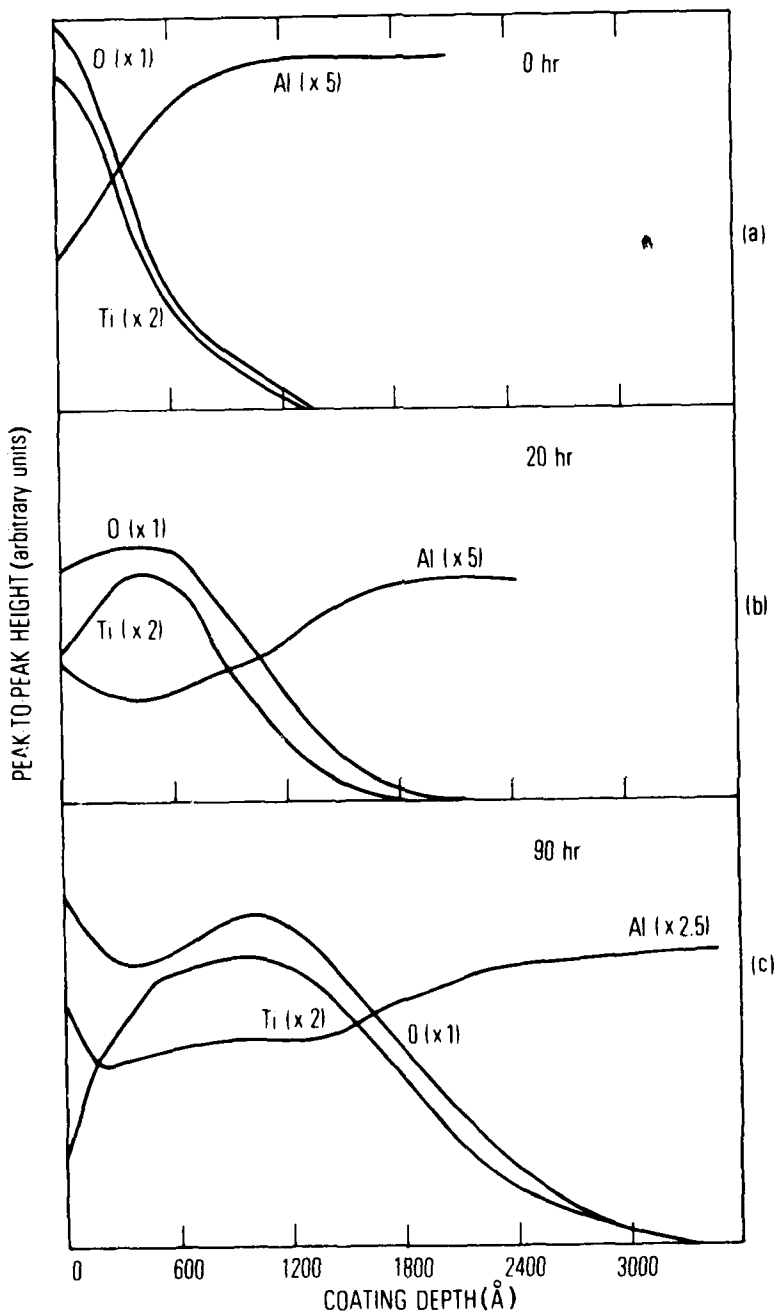

Fig. 24. Corrosion of a Mixed Coating Formed from TBT. (a) Before corrosion; (b) After 20 hr; (c) After 90 hr in salt-fog chamber

then oxidized, probably by water (Ref. 32) or oxygen, and the remaining titanium acts to increase the conductivity. In terms of our original model for corrosion resistance (see Section III), the TiO_2-x system is not optimum because it is an oxide with a generally high concentration of defects (i.e., oxygen vacancies). The occurrence of defects is usually associated with increased conductivity; TiO_2 is, in fact, a defect semiconductor (Ref. 21). The aluminum and oxygen content of the coating increases during corrosion as does the coating thickness. Finally, the porosity of the developing aluminum oxide layer causes discoloration of the aluminum. Pitting may occur at thin areas of the developing aluminum oxide coating. In our tests, discoloration of sample surface is defined as coating failure.

Corrosion lifetime as a function of coating thickness, of the polymeric condition of the original TBT, and of the humidity of the hydrolysis atmosphere, is illustrated in Fig. 25. Several trends are clear from this figure. Thin coatings (200 to 800 Å) that have poor corrosion resistance (less than 70 hr) result from coatings applied from wet or dry solutions of trimeric TBT and hydrolyzed at low humidity. Thicker (600 to 800 Å) coatings that have somewhat better corrosion resistance (about 80 hr) result from polymeric starting material hydrolyzed at low humidity. A wide range of humidities is included under the wet humidity designation, which accounts for the wide range of the data. Trimeric TBT hydrolyzed in humid atmospheres results in thick coatings (600 to 2000 Å) and good corrosion resistance (50 to 90 hr). High humidity and the use of prepolymerized TBT result in superior mixed oxide coatings that have thicknesses of 1000 to 1700 Å and salt-fog spray corrosion lifetimes of 90 to 130 hr whether the bath is wet or dry. The following conclusions are drawn from these data: (a) prepolymerized TBT results in thick coatings regardless of humidity; and (b) corrosion resistance and coating thickness improve with increased humidity in the hydrolysis atmosphere.

B. COATINGS ON ALUMINUM ALLOYS

Chromate and titanate coatings were deposited on three common structural aluminum alloys to assess the importance of minor alloy constitutents as

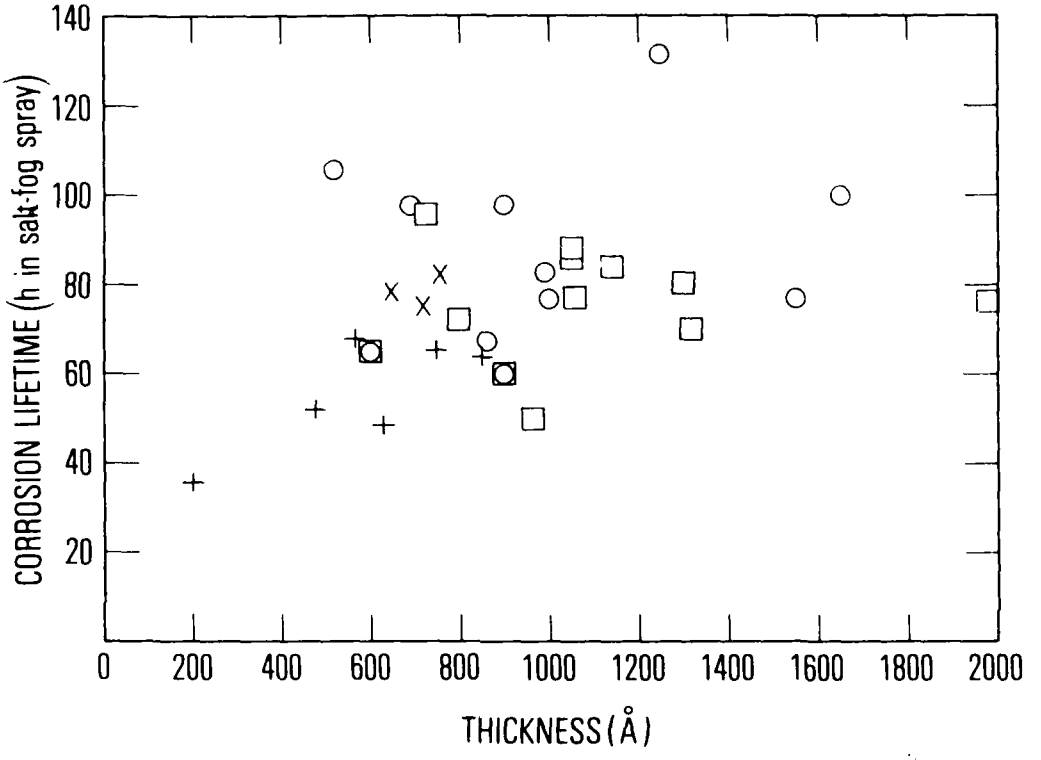

Fig. 25. Effect of Prepolymerization and Hydrolysis Atmosphere on Corrosion Resistance. Coatings applied as trimeric TBT and hydrolyzed at high humidity (□) or low humidity (+). Coatings applied as prepolymerized TBT and hydrolyzed at high humidity (O) or low humidity (x)

determinants of corrosion resistance. The magnesium-silicon-aluminum alloy AA 6061 is generally considered to have good corrosion resistance and moderate strength. The aluminum-copper alloy AA 2024, and the aluminum-zinc-magnesium alloy AA 7075, have higher strengths but generally poor corrosion resistance. Both alloys are used in aircraft construction. Alloy compositions are given in Table 11.

The chromate coatings once again provide a standard against which to judge the effectiveness of our organometallic coating formulations. The salt-spray results presented in Table 12 indicate that the STC chromate coating affords corrosion protection to the aluminum alloys investigated; however, the corrosion resistance of the coated alloys is notably less than that of coated, commercially pure aluminum. The corrosion resistance of a structural alloy generally decreases as the content of minor alloy constitutents increases. This unfortunate trend is attributed to the formation through segregation of regions of different electrochemical potential and resultant galvanic corrosion.

1. EFFECT OF COPPER

We have already discussed the effect on corrosion resistance of residual surface copper remaining after the application of different cleaning procedures to high purity and to commercially pure aluminum. Copper also plays a dominant role in determining the corrosion resistance of structural aluminum alloys. The salt spray environment is quite aggressive to uncoated aluminum, but it is evident from the data in Table 12 that commercially pure aluminum (AA 1100) is more resistant than the alloys listed, and that, among the alloys, AA 6061 has the best corrosion resistance. Differences in corrosion resistance are pronouced for most coating types on the various alloy substrates, but again coated AA 6061 in general exhibits greater corrosion resistance than do the other alloys covered by the same coating. Alloy AA 6061 has a lower copper content than either AA 2024 or AA 7075.

On the basis of our conceptual picture of protective surface oxides, copper should adversely affect coating corrosion resistance. Copper has two oxidation states and should serve to increase the electrical conductivity of

Table 12. Summary of Alloy Salt Spray Corrosion Data for Different Specimen Treatments[a]

Pretreatment,[b] Coating	Alloy Designation, AA No. 1100	2024	6061	7075
Baseline Data				
C Uncoated	18	10	15	10
C Uncoated	19	9	19	8
C,P Uncoated	20	13	15	12
C STC	260	90	113	95
C,P STC	480	45	360	80
TBT Coatings[c]				
C TBT (fresh)	29	10	23	10
C TBT (24 hr; 0.2% H_2O)	110	11	63	10
C TBT (6d; 0.2% H_2O)	88	10	39	10
C TBT (24 hr; 0.1% H_2O)	69	10	58	14
C TBT (24 hr; 0.1% H_2O); 150° overnight	72	14	86	12
Organic Inhibitors				
C $N(C_2H_4OH)_3$ + TBT	71	14	71	13
C $(CH_3)_2$ NH + TBT	46	16	46	16
C $HCON(CH_3)H$ + TBT	76	14	68	13
C TBT + $HCONCH_3H$	131	16	115	16
C HOC_2H_4SH + TBT	137	16	137	16
C HOC_2H_4SH + TBT	76	13	48	12
C HOC_2H_4SH (no TBT)	44	12	36	12

[a] Table entries are times required to reach a given degree of corrosion as determined with reference to an arbitrary visual scale. Each entry represents an average over eight test coupons.

[b] C = cleaned (see Section V.A); P = chemically polished.

[c] First number in parentheses indicates time interval between TBT solution preparation and coating application. Second number (when given) is the concentration of H_2O (wt %) in the coating solution.

oxide coatings. A simple galvanic mechanism, however, with the copper nonuniformly distributed on the surface, could also account for the deleterious effect of copper on corrosion resistance. The spatial resolution of the scanning Auger microprobe was not sufficient to preclude the latter possibility.

2. EFFECT OF MAGNESIUM

An Auger depth profile shows that uncoated AA 6061 (chromate cleaned) is enriched in surface magnesium (15 wt% magnesium etc.) (Fig. 26). The composition as determined by AES is consistent with the presence of $MgAl_2O_4$, or with a simple mixture of magnesium and aluminum oxides. Both Auger and IMMA depth profiles of the surface oxide after application of a TBT coating show significant diffusion of magnesium into the oxide coating. Note that the TBT coating of magnesium-rich AA 6061 surfaces does not result in a magnesium-rich interfacial region between the coating and the substrate AA 6061, but rather yields a coating which contains large amounts of distributed magnesium. The magnesium is concentrated on the surface of the oxide coating, and the concentration drops to the bulk alloy value as the oxide coating is sputter profiled.

It is known that heating magnesium-containing alloys (e.g., AA 2024) in air at 150°C for 3 hr will result in segregation of magnesium at the surface (Ref. 38). Heating a TBT-coated and hydrolyzed AA 6061 coupon at 150°C for 12 hr in air produces no concentration of magnesium in the titanium oxide coating above that found for similarly coated but unheated samples. The mobility of magnesium in the titanium oxide coating after hydroysis thus appears to be low. These observations, that magnesium does not diffuse through the titanium oxide coating from the bulk substrate when heated after hydrolysis and is not concentrated in the interfacial region between the titanium oxide and substrate alloy, suggest that the transfer of magnesium to the surface of the titanium oxide coating must take place while the titanium is in the unconsolidated "gel" state. The hydrated surface magnesium oxide apparently has some solubility in the gel, in contrast to the case of copper where diffusion of copper through the gel does not occur.

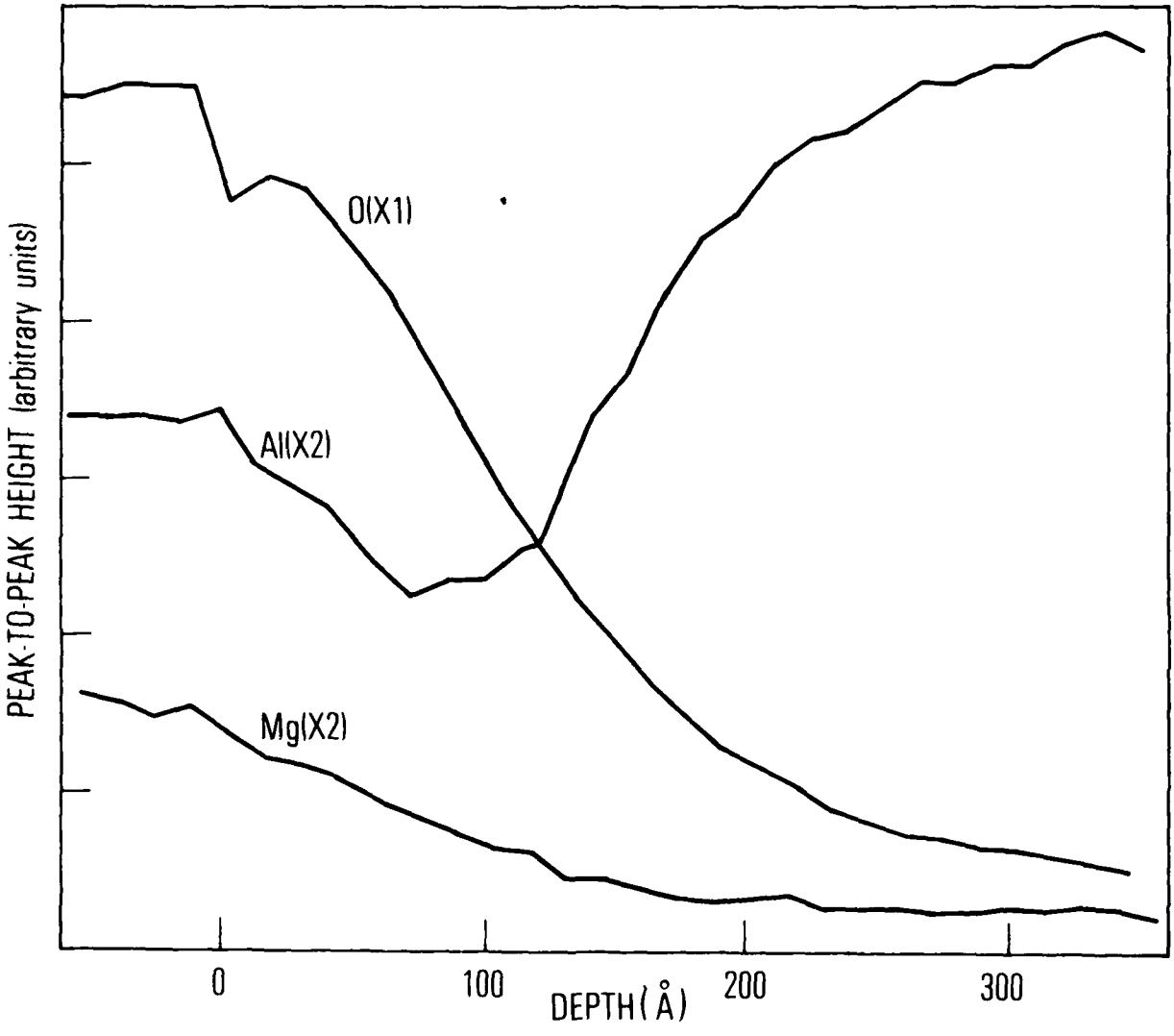

Fig. 26. Auger Depth Profile, AA 6061 Alloy, Chromate Cleaned

As a general rule, magnesium in a bulk alloy tends to have a beneficial effect on corrosion resistance (Ref. 39). Our study shows a beneficial effect resulting specifically from magnesium within the oxide layer. Some correlation is inferred between coating magnesium content, as determined from IMMA data, and salt spray corrosion resistances (Fig. 27). This role of magnesium in enhancing coating corrosion resistance is of particular interest since our conceptual model indeed predicts that divalent cations, such as magnesium, should enhance corrosion resistance. Magnesium, having but one formal charge state, will not promote electronic conductivity and will compensate for oxygen vacancies.

3. EFFECT OF ORGANIC INHIBITORS

We examined the effects of organic corrosion inhibitors in order to gain further insight into the role of impurities. It has long been known that corrosive attack in different environmental media is reduced by the addition of certain organic compounds. These corrosion inhibitors are usually sulfur or nitrogen compounds and are usually good metal complexing ligands with both, hydrophobic and hydrophilic parts. It is believed that the hydrophilic portion of the molecule attaches to the surface, while the hydrophobic portion is oriented toward the surrounding medium and blocks interaction with the medium. We applied several organic compounds on AA 6061 to determine if we could confirm details of our model by demonstrating that improved corrosion resistance is associated specifically with the immobilization or isolation of copper. Most of the test compounds applied in conjunction with Tyzor TBT yielded coatings with salt-spray lifetimes only equal to (or less than) ordinary TBT coatings (Table 12). However, we did find two systems with dramatically improved corrosion resistance, actually superior to STC chromate coating for this particular alloy.

One such system involves mercaptoethanol. When AA 6061 is first treated by immersion in mercaptoethanol and then coated with Tyzor TBT, Auger depth profile analysis (Fig. 28) shows sulfur on the oxide surface, with sulfur concentration decreasing into the coating. There is no concentration of sulfur at the substrate coating interface. X-ray photoelectron spectroscopy

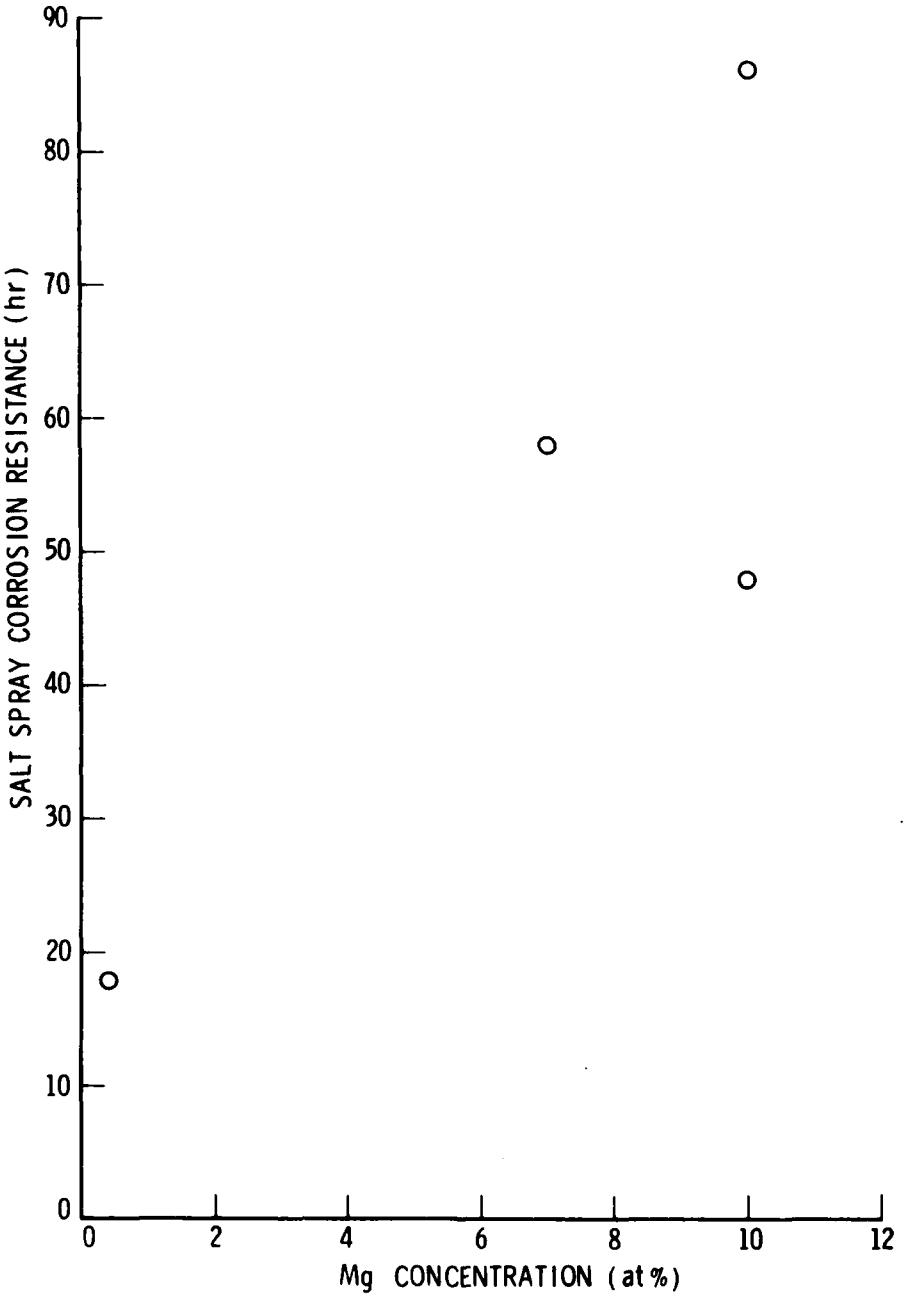

Fig. 27. Corrosion Resistance vs Surface Magnesium Concentration for AA 6061 Plus TBT

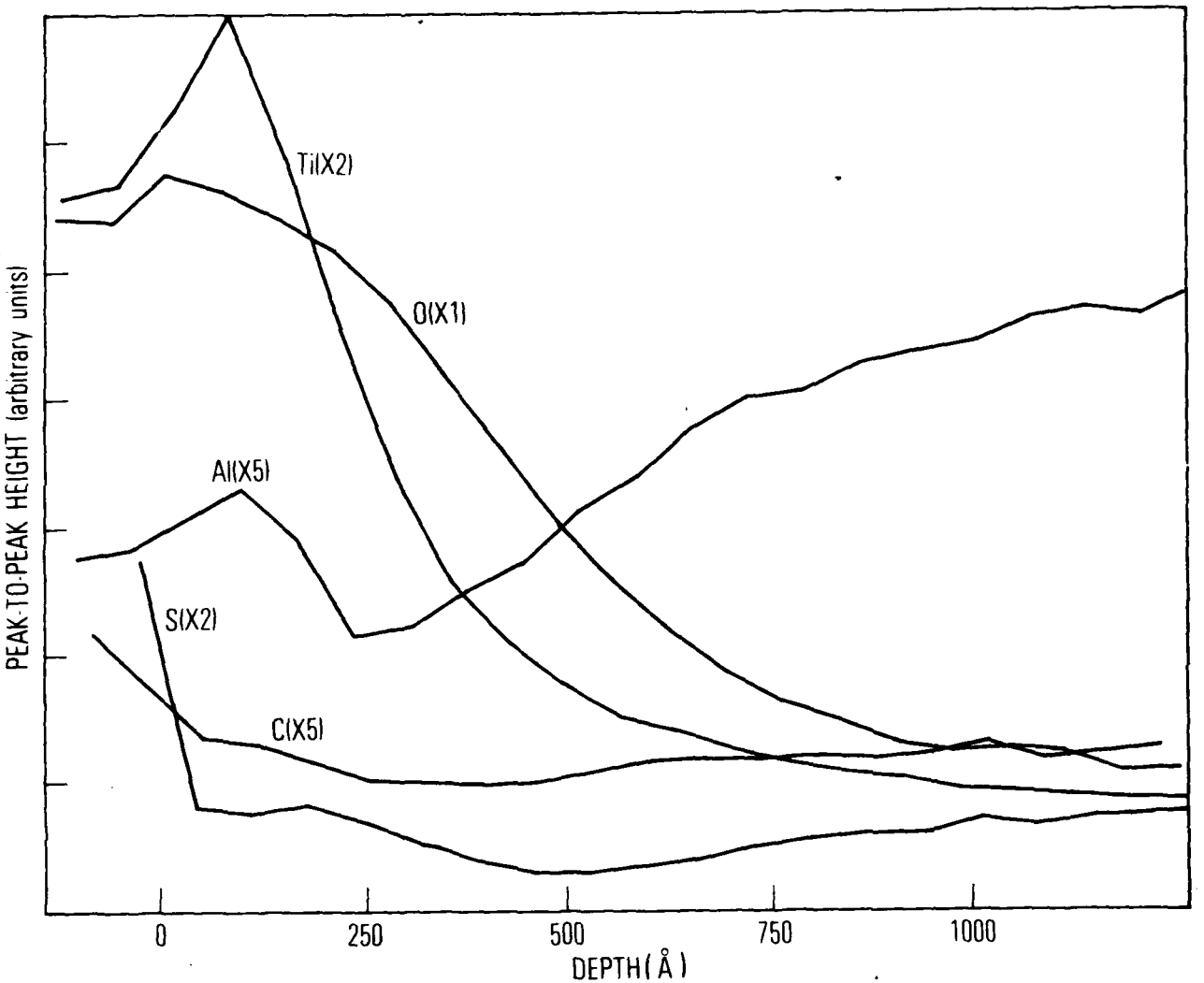

Fig. 28. Auger Depth Profile, AA 6061 Alloy, Mercaptoethanol Plus TBT

shows that the mercaptan (SH) functional group is oxidized to a sulfate or sulfuryl group. Diffusion of sulfur must take place in the gel phase prior to coating hydrolysis.

Methylformamide provides an interesting contrast to the case of mercaptoethanol. If AA 6061 is first coated with methylformamide, then coated with Tyzor TBT, no improvement in corrosion resistance is noted. However, coating with TBT, followed by hydrolysis and treatment with methylformamide, results in a superior corrosion-resistant coating. X-ray photoelectron spectroscopy analysis does not reveal any surface nitrogen, and Auger depth profile analysis reveals no features that would account for improved corrosion resistance.

VIII. SUMMARY AND CONCLUSIONS

The basic goals of our research program, as outlined in the original proposal, have been accomplished.

Our examination of the chromate coating system resulted in an understanding of the critical role of either OH^- or HF in the initial dissolution of surface oxide. The details of film structure were found to depend on relative rates of formation and dissolution of AlOOH and CrOOH. The chromate coating formulations stand as a movement to the empirical method. Systematic variation of coating parameters, combined with coating characterization using modern surface analysis instrumentation, did not yield a chromate coating superior to those formed from recipes developed over 50 years ago.

The titanate coatings have served as useful model systems for the investigation of the new class of mixed oxide coatings deposited from nonaqueous solutions of organometallic compounds. We anticipated the formation of uniform, distinct mixed oxide phases under the conditions of our experiments. Uniform phases would of course be discernable in Auger depth profile analyses as regions of constant composition. Such regions were not found in any of the systems studied. Oxide composition for deposited coatings changes continously. This observation is not, however, incompatible with our conceptual picture of oxide structure. In fact, our experimental observations on all oxide systems are compatible with our original conceptual picture. Evidence tending to confirm our model includes the deleterious effect of monovalent impurities (copper) on corrosion resistance and the apparently benevolent effect of divalent cations (magnesium). Furthermore, increased corrosion resistance is associated with increased thickness of the mixed oxide region.

The development of a coating formulation for AA 6061 to be more corrosion resistant than the STC chromate coating is potentially significant for practical corrosion protection technology. Although this particular path of investigation was suggested by our model, the interaction of inhibitory sulfur and nitrogen compounds with oxide coatings to improve corrosion resistance is not yet understood in detail.

It should again be pointed out that titanium oxide was chosen as a model system for the specific reasons cited earlier. Titanium dioxide is, however, a defect semiconductor and is not in principle the optimum protective oxide.

We do suggest that the use of mixed oxide systems, in combination with an "inhibitory" compound, offers an opportunity to develop very useful practical coatings. Further study is needed to better understand the synergistic interaction between surface oxide layers and inhibitory compounds. It remains to be determined whether the oxide coating itself is affected or whether the coating simply provides a suitable substrate for the inhibitors. It is also essential that the work be extended to encompass aircraft structural alloys.

REFERENCES

1. H. A. Katzman, G. M. Malouf, R. Bauer, and G. W. Stupian, "Corrosion-Protective Chromate Coatings on Aluminum," Applications of Surface Science 2, 416-432 (1979).

2. R. A. Lipeles, G. M. Malouf, P. D. Fleischauer, and G. W. Stupian, "The Formation of Corrosion Protective Mixed Aluminum-Titanium Oxide Films from Tetrabutyl Titanate," submitted to Applications of Surface Science (1980).

3. G. W. Stupian, "Multicomponent Oxide Systems for Corrosion Protection," a research proposal submitted to the Air Force Office of Scientific Research, The Aerospace Corporation, El Segundo, Calif. (1977).

4. G. W. Stupian, P. D. Fleischauer, H. A. Katzman, and G. M. Malouf, Annual Report: Multicomponent Oxide Systems for Corrosion Protection, ATR-78(7679)-2, The Aerospace Corporation, El Segundo, Calif. (1978).

5. G. W. Stupian and R. A. Lipeles, Annual Report: Multicomponent Oxide Systems for Corrosion Protection, 1 July 1978 - 30 June 1979, ATR-79(7679)-1, The Aerospace Corporation, El Segundo, Calif. (1979).

6. T. A. Carlson, Photoelectron and Auger Spectroscopy, Plenum Press, New York (1975).

7. L. E. Davis, N. C. MacDonald, P. W. Palmberg, G. E. Riach, and R. E. Weber, Handbook of Auger Electron Spectroscopy, 2nd ed., Physical Electronics Ind., Edina, Minn. (1976).

8. T. A. Whatley and E. Davidson, Ion Microprobe in Systematic Materials Analysis, Vol. 4, J. H. Richardson and R. V. Peterson, eds., Academic Press, New York (1978).

9. R. T. Sanderson, Inorganic Chemistry, Reinhold, New York (1967).

10. S. Wernick and R. Pinner, Surface Treatment of Aluminum, Vol. 1, 4th ed., Robert Draper, Ltd., Teddington (1972), pp. 233-290.

11. R. J. Sunderland, Japan J. Appl. Phys., Suppl. 2, Pt. 1 (1974) 347.

12. J. A. Treverton and N. C. Davies, Metals Tech. 4 (1977) 480.

13. D. T. McDevitt, W. L. Baun, and J. S. Solomon, AFML-TR-75-122, Air Force Materials Laboratory (1975).

14. A. Pattnaik and J. D. Meakin, Report No. FC3632, Franklin Institute Research Laboratories (1974).

15. M. F. Abd Rabbo, J. A. Richardson, and G. C Wood, Corrosion Sci. 18 117 (1978).

16. G. K. Wehner, The Aspects of Sputtering in Surface Analysis Methods, in: Methods of Surface Analysis, ed. A. W. Czanderna; Elsevier, Amsterdam (1975).

17. G. Eckert, Aluminum 19 608 (1937).

18. W. Marchand, Electroplating and Metal Finishing 14 439 (1961).

19. M. Pourbaix, Atlas of Electrochemical Equilibria in Aqueous Solution (National Association of Corrosion Engineers, Houston, 1974).

20. T. Valand and G. Nilsson, Corrosion Sci. 17 449 (1977).

21. M. J. Dignam, Mechanisms of Ionic Transport through Oxide Films, in: Oxides and Oxide Films, Vol. 1, ed. J. W . Diggle, Marcel Dekker, New York (1972), pp. 92-286.

22. R. L. Martin and G. Winter, J. Chem. Soc. 2947 (1961).

23. N. M. Cullinane, S. J. Chard, G. F. Price, B. B. Millward, and G. Langlois, J. Appl. Chem. 1, 400 (1951).

24. S. Minami and T. Ishino, Technol. Rept., Osaka Univ. 3 357 (1953).

25. C. N. Caughlan, H. S. Smith, W. Katz, W. Hodgson, and R. W. Crowe, J. Amer. Chem. Soc. 73, 5652 (1951).

26. D. C. Bradley, R. C. Mehrotra, J. D. Swanwick, and W. Wardlaw, J. Chem. Soc. 2025 (1953).

27. D. C. Bradley, R. Gaze, and W. Wardlaw, J. Chem. Soc. 469 (1955); 721, 3977 (1955).

28. D. C. Bradley and C. E. Holloway, Inorg. Chem. 3, 1163 (1964).

29. G. Winter, Oil and Colour Chemist's Assoc. 36 689 (1953).

30. T. Boyd, J. Polymer Sci. 7, 591 (1951).

31. L. M. Brown and K. S. Mazdiyasni, Inorg. Chem. 9 2783 (1970).

32. B. F. Thompson, J. Council Sci. Ind. Research, 19, 157 (1946).

AD-A099 995 AEROSPACE CORP EL SEGUNDO CA LAB OPERATIONS F/G 11/3
MULTICOMPONENT OXIDE SYSTEMS FOR CORROSION PROTECTION,(U)
NOV 80 G W STUPIAN, P D FLEISCHAUER AFOSR-77-3334
UNCLASSIFIED ATR-81(7679)-1 AFOSR-TR-81-0472 NL

33. M. S. Hunter and P. Fowler, J. Electrochem Soc. 103, 482 (1957).

34. H. J. Mathieu, D. E. McClure, and D. Landolt, Thin Solid Films 38, 281 (1976).

35. H. A. Clark, "Pigment Free Coating Compositions," U.S. Patent 4,027,073 (31 May 1977).

36. C. D. Wagner, W. M. Riggs, L. E. Davis, J. F. Moulder, and G. E. Muellenberg, Handbook of X-ray Photoelectron Spectroscopy, Perkin-Elmer Corp., Physical Electronics Division, Eden Prairie, Minn. (1979).

37. F. A. Cotton and G. Wilkinson, Advanced Inorganic Chemistry, 3rd ed., Interscience Publishers, New York (1972), p. 52.

38. T. S. Sun, J. M. Chen. J. D. Venables, and R. Hopping, Applic. of Surf. Sci. 1, 202 (1978).

39. H. P. Goddard, W. B. Jepson, M. R. Bothwell, and R. L. Kane, The Corrosion of Light Metals, John Wiley and Sons, New York (1967).

APPENDIX

PUBLICATIONS AND PRESENTATIONS

All program publications and interactions performed in accordance with grant reporting requirements are listed herein. Most publications were also referenced in the text.

Publications in the open literature:

H. A. Katzman, G. M. Malouf, R. Bauer, and G. Stupian, "Corrosion-Protective Chromate Coatings on Aluminum," Applications of Surface Science 2, 416-432 (1979).

Future publications:

1. R. A. Lipeles, G. M. Malouf, P. D. Fleischauer, and G. W. Stupian, "The Formation of Corrosion Protective Mixed Aluminum-Titanium Oxide Coatings from Tetrabutyl Titanate," (to be published).

2. "A Survey of Possible Mixed Oxide Systems for Corrosion Protection" (to be submitted to Corrosion Science).

Presentations:

Dr. G. W. Stupian was dinner speaker at a meeting of the Thin Films and Surfaces Chapter, Southern California Section, American Vacuum Society, on August 6, 1980, and presented a talk entitled "Mixed Oxide Systems for Corrosion Protection."


DATE
FILME